Near-Road Particulate Pollution: $PM_{2.5}$, Black Carbon, and Ultrafine Particles at U.S. Near-Road Monitoring Sites

Analysis of near-road $PM_{2.5}$, black carbon, and ultrafine particle monitor concentrations and the potential contribution from roadways.

TxDOT Environmental Affairs Division
Date: December 2019
200.05.GUI

Near-Road Particulate Pollution: $PM_{2.5}$, Black Carbon, and Ultrafine Particles at U.S. Near-Road Monitoring Sites

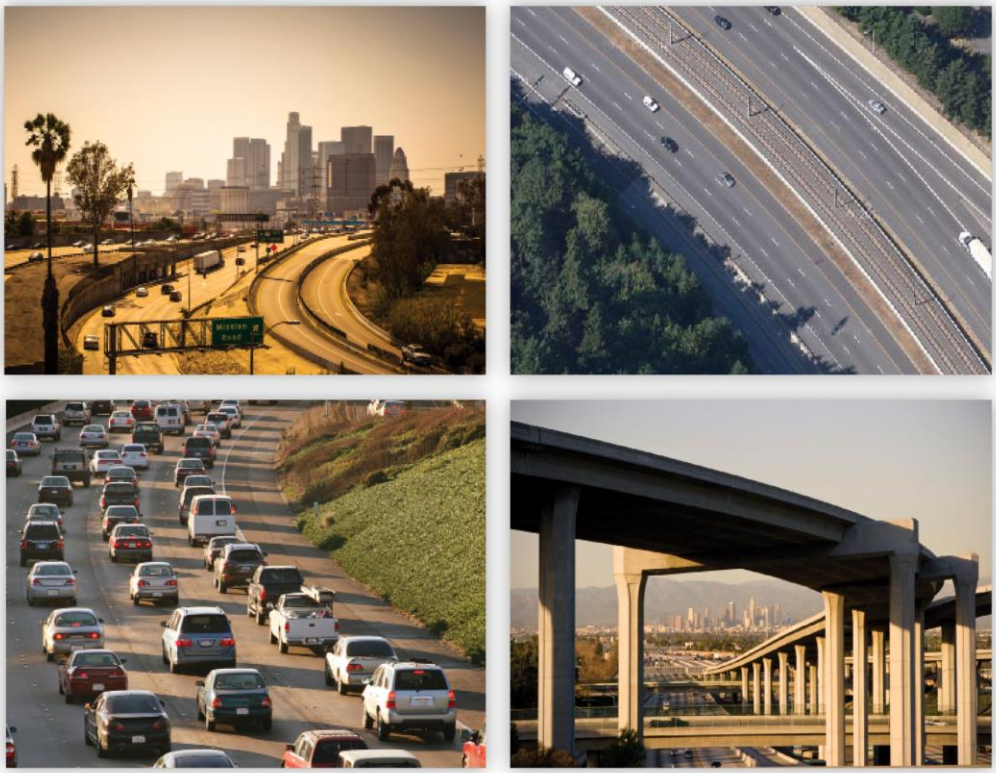

Final Report prepared for

Texas Department of Transportation
Austin, TX

December 2019

STi | Sonoma Technology

This document contains blank pages to accommodate two-sided printing.

Near-Road Particulate Pollution: $PM_{2.5}$, Black Carbon, and Ultrafine Particles at U.S. Near-Road Monitoring Sites

Prepared by

Anondo Mukherjee, PhD
Olivia Ryder, PhD
Mike McCarthy, PhD
Steve Brown, PhD
Douglas Eisinger, PhD

Sonoma Technology, Inc.
1450 N. McDowell Blvd., Suite 200
Petaluma, CA 94954-6515
Ph 707.665.9900 | F 707.665.9800
sonomatech.com

Prepared for

Jackie Ploch

Texas Department of Transportation
(TXDOT) Environmental Affairs Division
125 E. 11th Street
Austin, TX 78701-2483
512.416.3001
txdot.gov

Final Report

STI-914206-7208

December 31, 2019

Acknowledgments

The authors acknowledge Dr. Jonathan Wang, University of Toronto, for his generous help with the Igor code used in the time series BC analysis.

Contents

Figures vii
Tables viii
Terms ix

Summary 1

1. Introduction and Objectives 3
   1.1 Background 3
   1.2 Near-Road $PM_{2.5}$ 3
   1.3 Black Carbon and Ultrafine Particles 4
   1.4 Objectives 4

2. Methods 7
   2.1 Data Sources 7
      2.1.1 Air Quality Data and Near-Road Site Characteristics 7
      2.1.2 Meteorological Data 10
      2.1.3 Land Use 10
   2.2 $PM_{2.5}$ Increment Calculation 10
   2.3 BC Increment Calculation 11
   2.4 Comparison of Ambient Data with Site Characteristics 12

3. Results 13
   3.1 2018 $PM_{2.5}$ NAAQS Comparison for 52 Near-Road Sites 13
   3.2 2016-2018 $PM_{2.5}$ NAAQS Comparison for 26 Near-Road Sites 15
   3.3 Three-Year and Five-Year Annual Average $PM_{2.5}$ Trends at Near-Road Sites 16
   3.4 $PM_{2.5}$ Increments at Near-Road Sites Before Removal of Sites Affected by Confounding Factors 18
   3.5 $PM_{2.5}$ Increments at 32 Sites After Removal of Sites Affected by Confounding Factors 20
   3.6 Increment Comparison to Site Characteristic Variables 24
   3.7 Comparing 2018 and 2017 $PM_{2.5}$ Increments 27
   3.8 Near-Road Ultrafine Particle Concentrations 28
   3.9 Near-Road Black Carbon Concentrations 29
      3.9.1 Black Carbon Concentration Distributions 29
      3.9.2 Black Carbon Increments 34
      3.9.3 Black Carbon Fraction of $PM_{2.5}$ 38

4. Conclusions 41

5. References 43

Appendix: Supplementary Data 49

Figures

1. Distribution of daily average $PM_{2.5}$ at 52 near-road monitoring sites in 2018, sorted by annual mean 14
2. Distribution of daily average $PM_{2.5}$ at 26 near-road monitoring sites from 2016 to 2018, sorted by three-year average annual mean 15
3. Distribution and trends of annual average $PM_{2.5}$ at near-road monitoring sites 17
4. Distributions of annual average $PM_{2.5}$ increments using identical instrument methods from 46 near-road sites, computed using IDW and the nearest-monitor method 19
5. Distributions of 2018 annual average $PM_{2.5}$ increments computed using IDW and nearest-monitor calculation 23
6. Boxplot distributions of 2018 annual average $PM_{2.5}$ increments computed using IDW and nearest-monitor calculation 24
7. The relationship between the 2018 IDW $PM_{2.5}$ increment in comparison to distance to road, FE-AADT, percentage of time upwind of the roadway, and AADT 26
8. Box plot of 2016-2018 UFP concentrations by site under downwind, parallel, and upwind wind conditions 29
9. BC concentrations from 29 near-road sites under downwind, parallel, and upwind wind conditions during 2016-2018 31
10. Three year average (2016-2018) BC increments calculated from the time series method developed by Wang et al. (2018) for all 29 sites and the nearby monitor method for 16 sites where nearby monitor data were available 35
11. The relationship between the three year (2016-2018) average BC concentration and BC increment in comparison to distance to road 37
12. The relationship between the monitor distance to road and the BC fraction of $PM_{2.5}$, based on 2018 annual average values 40

Tables

1. Near-road sites measuring $PM_{2.5}$, BC, and UFP 8
2. Near-road site characteristics, 2018 increments, and increment uncertainties from the IDW and nearest-monitor methods for the 32 near-road sites 21
3. Coefficient of determination (R^2 value) for IDW and nearest-monitor increments with near-road site and meteorological variables for 2018 25
4. The intercepts, slopes, p-values, and R^2 values for the four regressions presented in Figure 7 26
5. Average BC concentrations and increments for the three-year period (2016-2018) 32
6. Coefficient of determination (R^2 value) of near-road site characteristics with BC concentrations and increments for 2016-2018 36
7. The intercepts, slopes, p values, and R^2 values for linear regressions predicting BC concentration and increment with distance to road 38
8. Annual average $PM_{2.5}$ and BC concentrations for 2018 for 20 near-road sites 39

Terms

Term	Definition
AQS	U.S. EPA's Air Quality System
BC	Black Carbon
CO	Carbon Monoxide
FE-AADT	Fleet-Equivalent Annual Average Daily Traffic
FEM	Federal Equivalent Method
FRM	Federal Reference Method
HDVs	Heavy-Duty Vehicles
IDW	Inverse Distance Weighting Squared Method
IQR	Inter-Quantile Range
NAAQS	National Ambient Air Quality Standards
NLCD	National Land Cover Database
NM	Nearby Monitor
NO_2	Nitrogen Dioxide
NO_x	Oxides of Nitrogen
$PM_{2.5}$	Particulate Matter 2.5 Micrometers in Aerodynamic Diameter or Smaller
R^2	Coefficient of Determination
UFP	Ultrafine Particle
USGS	United States Geological Survey
POAQC	Transportation Projects of Local Air Quality Concern

Summary

Major roadways are an important emission source of particulate pollution, through vehicle exhaust, brake and tire wear, and re-suspended road dust. We examined the concentrations of particulate matter 2.5 micrometers in aerodynamic diameter or smaller ($PM_{2.5}$), black carbon (BC), and ultrafine particle (UFP) counts from 58 near-road monitoring sites, focusing on 2016-2018 data. These sites represent a diverse range of conditions, with fleet-equivalent annual average daily traffic (FE-AADT) values ranging from approximately 126,000 to 631,000.

We present three-year (2016-2018) and five-year (2014-2018) trends of annual average $PM_{2.5}$ for near-road sites for which data are available. Sites with only three years of data did not show a consistent trend. Six of seven sites with five years of data showed a decreasing trend in annual average $PM_{2.5}$ levels. With the exception of six sites, 2018 daily average and annual average values were below the NAAQS standards—four of these six sites were substantially impacted by $PM_{2.5}$ from wildfires. When calculated using a U.S. Environmental Protection Agency–recommended inverse distance weighting squared (IDW) method, the near-road $PM_{2.5}$ increment, i.e., the difference between the near-road and background $PM_{2.5}$ concentrations, ranged from -0.14 ± 1.11 to 1.68 ± 0.91 μg/m^3 at sites with Federal Reference Method (FRM) monitors. With the exception of one near-road site with an increment of 2.49 ±1.42 μg/m^3, all other sites where Federal Equivalent Method (FEM) monitors were used had increments below 2.0 μg/m^3. Increments corresponded to a roadway contribution between 1% and 27% of total near-road $PM_{2.5}$. Increments have a statistically significant relationship with near-road site variables, including distance to the road and FE-AADT.

We examined UFP measurements from the 6 near-road sites and BC measurements from the 29 near-road sites for which data were available during 2016-2018. These measurements showed a clear diurnal pattern, with median concentrations peaking during morning hours (between 5:00 a.m. and 9:00 a.m.). Weekday UFP and BC concentrations were higher than weekend concentrations at all sites. The median UFP and BC values were typically higher when the monitor was downwind of the target roadway, than during upwind conditions. BC increments ranged from -0.02 to 1.2 μg/m^3, corresponding to a roadway contribution of between 37% and 78% of near-road BC. Near-road total annual average BC concentrations from 20 sites in 2018 ranged from 0.59 to 1.53 μg/m^3, which made up between 6.1% and 17.9% of total $PM_{2.5}$. The near-road site variables that were most correlated with the $PM_{2.5}$ increment and the BC increment were the monitor distance from the road, FE-AADT, and the percentage of time the monitor was upwind of the target road. The monitor distance from the target road was the variable with the strongest correlation with particulate concentrations and increments.

1. Introduction and Objectives

1.1 Background

Traffic-related emissions contribute to particulate pollution through direct emissions, such as exhaust, brake wear and tire wear, and through the emission of precursor gases that form particles 2.5 micrometers or smaller in aerodynamic diameter ($PM_{2.5}$) through gas-to-particle conversion. $PM_{2.5}$ mass has been shown to be higher next to a major roadway than at other nearby locations, although near-road concentrations are typically dominated by urban background (Seagram et al., 2019b; Hilker et al., 2019; Jeong et al., 2019; Sofowote et al., 2018). Black carbon (BC) and particle count (typically measured as ultrafine particles [UFP] less than 100 nm in diameter) may be 50% to 200% higher next to a roadway (Karner et al., 2010). For example, a recent study of three near-road monitoring stations sited between 6 and 15 meters from their target roadway in Toronto and Vancouver estimated that on-road emissions contributed between 15% and 35% of near-road $PM_{2.5}$ (Dabek-Zlotorzynska et al., 2019).

Since 2014, long-term measurements of pollutants next to major roadways in the U.S. have been made as part of EPA's update to the NO_2 National Ambient Air Quality Standards (NAAQS) in 2010 (U.S. Environmental Protection Agency, 2010). Previous studies have examined measurements of carbon monoxide (CO), nitrogen dioxide (NO_2) and $PM_{2.5}$ from these near-road monitors for data collected through 2017, as well as more detailed case studies of individual monitors (Seagram et al., 2019b; DeWinter et al., 2018; Brown et al., 2019; Mukherjee et al., 2019). To date, BC and UFP measurements at these U.S. near-road sites have not been examined.

1.2 Near-Road $PM_{2.5}$

Near-road $PM_{2.5}$ has been the subject of recent studies due to the importance of on-road emissions and the proximity of substantial metropolitan populations to major roadways (Dabek-Zlotorzynska et al., 2019; Abu-Allaban et al., 2007; Rowangould, 2013). Quantifying near-road $PM_{2.5}$ is also relevant for assessing the air quality impact of current and future transportation projects, within the context of regulatory requirements (Mukherjee et al., 2019; U.S. Environmental Protection Agency, 2015a). Studies have examined the gradients of $PM_{2.5}$ from the roadway, the meteorological and traffic conditions that lead to enhanced near-road $PM_{2.5}$ concentrations, and the fraction of near-road $PM_{2.5}$ attributable to traffic-related emissions (Karner et al., 2010; Baldwin et al., 2015; Brown et al., 2019; Dabek-Zlotorzynska et al., 2019; Clayton et al., 2003; Hilker et al., 2019; Wang et al., 2018). Emissions from heavy duty diesel vehicles are an important contributor of total $PM_{2.5}$ (Gertler, 2005).

The $PM_{2.5}$ increment represents the impact of traffic-related emissions. The $PM_{2.5}$ increment, defined as the difference between near-road $PM_{2.5}$ and a background estimate, was quantified using 2015

and 2016 data from EPA-mandated monitors by DeWinter et al. (2018) and Seagram et al. (2019a), respectively. The highest annual average $PM_{2.5}$ increment in 2017 from 40 near-road sites was 2.12 µg/m^3 (Mukherjee et al., 2019). One challenge in quantifying the $PM_{2.5}$ increment attributable to near-scale roadway emissions is that its magnitude is typically a small fraction of total $PM_{2.5}$ (Dabek-Zlotorzynska et al., 2019; Askariyeh et al., 2019; DeWinter et al., 2018; Seagram et al., 2019a; Mukherjee et al., 2019; Karner et al., 2010). Different methods have been used to estimate the background $PM_{2.5}$ levels, including time series analysis, choosing the most representative ambient monitor, and spatially weighting nearby ambient monitors (Seagram et al., 2019a; Wang et al., 2018).

1.3 Black Carbon and Ultrafine Particles

BC is produced in combustion processes, such as vehicle exhaust or wood combustion (Janssen et al., 2012). In the United States, the transportation sector contributes to the majority of BC emissions, with other important sources being open biomass burning such as wildfires, stationary power generation, industrial emissions, and residential biofuel use (Long et al., 2013). Near roadways, the main source of BC is exhaust emissions (Wang et al., 2011). For example, in Detroit, Baldwin et al. combined measurements and statistical modeling to determine a near-road increment of 0.24 µg/m^3 for BC and 2245 particles/cm^3 for UFP above urban background within 50 m of major roadways (Baldwin et al., 2015).

UFPs dominate total particle number counts in ambient air but contribute little to $PM_{2.5}$ mass overall (de Jesus et al., 2019; Health Effects Institute, 2013). In urban areas, UFPs are predominantly from mobile source emissions (Riddle et al., 2008; Marmur et al., 2006; Kleeman et al., 2009; Kulmala et al., 2004; Kumar et al., 2014; Salma et al., 2014; Harrison et al., 2011). UFPs can be emitted directly from combustion, or formed in the atmosphere via nucleation or condensation on pre-existing particles (Németh et al., 2018; Kulmala et al., 2004; Holmes, 2007; Brines et al., 2015; Salma et al., 2014; Canagaratna et al., 2010; Robinson et al., 2007). UFP concentrations are typically highest next to roadways, especially roadways with a higher number of heavy-duty vehicles (HDVs) (Harrison et al., 2011), and rapidly fall off within 100-300 m of the roadway, with strong spatial gradients within cities (Venecek et al., 2019; Karner et al., 2010; Zhu et al., 2002). Concentrations at urban locations in the 2000s decade were 7-11 x 10^3 particles/cm^3 for urban areas and 35-48 x 10^3 particles/cm^3 for a range of roadside or street canyon monitoring sites (Health Effects Institute, 2013; Morawska et al., 2008); lower levels were reported by de Jesus et al. (roughly 15-20 x 10^3 particles/cm^3 for roadside sites), using data from cities across the world (de Jesus et al., 2019).

1.4 Objectives

The objectives of this study were to (1) compare 2016-2018 near-road $PM_{2.5}$ measurements to NAAQS, (2) assess the 2018 annual average near-road increment for $PM_{2.5}$; (3) quantify near-road UFP and BC concentrations and increments; and (4) assess the relationship of both concentrations

and increments with site-specific factors such as traffic volumes and distance to road. Annual average $PM_{2.5}$ concentrations and increments for 2014 through 2017 from these near-road sites were previously reported (Seagram et al., 2019b; Mukherjee et al., 2019; DeWinter et al., 2018). To our knowledge, this is the first assessment of multiple years of near-road BC and UFP data from multiple near-road sites in the United States. Comparisons made to NAAQS in this report are for research purposes only and are not for air quality attainment status; U.S. EPA makes attainment-related determinations.

2. Methods

2.1 Data Sources

$PM_{2.5}$, BC, UFP, and meteorological data were downloaded directly from EPA's Air Quality System (AQS) for all monitoring sites in the U.S. for 2016-2018. Near-road site data and associated metadata (distance of monitor to roadway, traffic volume, AQS site identifier codes) were acquired from EPA's near-road website (https://www3.epa.gov/ttnamti1/nearroad.html). When meteorological data at a near-road site were not available, nearby meteorological data from an ambient station or the MesoWest database were used. Land use data were adapted from the National Land Cover Database (NLCD), developed by the United States Geological Survey (USGS).

2.1.1 Air Quality Data and Near-Road Site Characteristics

Monitoring sites in this study are identified by their city and the last four digits of their EPA AQS site ID codes, since some cities have multiple near-road sites (e.g., Philadelphia-0075 and Philadelphia-0076). The EPA near-road metadata provide the geographic coordinates of the monitor and the distance of the near-road monitor from the target road, defined as the distance to the edge of the roadway. The EPA metadata contain AADT and fleet-equivalent AADT (FE-AADT) information for the target road from the year 2016. EPA developed the FE-AADT calculation to represent an emissions-weighted traffic volume, taking into account both AADT and fleet mix (U.S. Environmental Protection Agency, 2012). FE-AADT is calculated as:

$$(AADT - HD_c) + (HD_m \times HD_c)$$

where HD_c is the volume of heavy-duty vehicles on the target roadway, and HD_m is a scaling factor that represents the ratio of heavy-duty to light-duty emissions of oxides of nitrogen (NO_x).

In assessing $PM_{2.5}$ data, we filtered for sites that had $PM_{2.5}$ data with over 75% annual completeness in 2018 in at least three out of four quarters (Jan-Mar, Apr-Jun, Jul-Sep, Oct-Dec). Data with specific qualifier flags to indicate quality assurance errors or exceptional events were excluded from this analysis. Near-road sites with multiple collocated records were classified by instrument method type: federal reference method (FRM) or federal equivalent method (FEM). The FRM measurements used in this study are based on 24-hour filter sampling and measure $PM_{2.5}$ through gravimetric techniques. The FEM measurements used in this study are based on hourly samples with instruments that use gravimetric or beta-attenuation techniques to measure $PM_{2.5}$. Where both existed, we used FRM data in lieu of FEM. If multiple FRM records or multiple FEM records were available at a near-road site, the one with more days of data was chosen. As shown in **Table 1**, 52 near-road sites had a complete $PM_{2.5}$ record for 2018. Hourly BC measurements were available at 29 near-road sites, and hourly UFP

data were available at six near-road sites from 2016 to 2018. $PM_{2.5}$ data for 2018 were available for 52 near-road sites; for these sites, we compared data to the NAAQS using only 2018 measurements. Of these 52 near-road sites, 26 sites have measurements from 2016-2018 that met completeness thresholds for each year; for these 26 sites, we compared 2016-2018 data to the NAAQS and evaluated three-year trends. Of these 26 sites, 7 sites have measurements from 2014-2018 that met completeness thresholds for each year; for these sites, we also evaluated five-year trends.

Table 1. Near-road sites measuring $PM_{2.5}$, BC, and UFP. Distance to road, AADT, and FE-AADT are shown for sites with available data. The number of $PM_{2.5}$ days is from 2018, and the number of BC and UFP hours are from 2016-2018. A distance of zero to a meteorology site designates collocated measurements.

Site Name	State	AQS ID	Distance to Road (m)	AADT	FE-AADT	N $PM_{2.5}$ Days	N BC Hours	N UFP Hours	Distance to Meteorology Site (km)
Atlanta-0003	GA	13-089-0003	35	147,000	320,710	NA	17484	NA	2
Atlanta-0056	GA	13-121-0056	7	382,000	544,678	121	17484	NA	0
Austin-1068	TX	48-453-1068	43	144,013	268,441	86	NA	NA	0
Berkeley-0013	CA	06-001-0013	19	267,000	382,108	363	17160	NA	17.9
Birmingham-2059	AL	01-073-2059	25	126,670	193,362	61	NA	NA	0
Boston-0044	MA	25-025-0044	10	205,861	261,441	355	25198	NA	2.2
Charlotte-0045	NC	37-119-0045	36	154,000	262,535	56	NA	NA	0
Cheektowaga-0023	NY	36-029-0023	20	126,107	212,275	116	16145	24412	6.1
Chelmsford-0010	MA	25-017-0010	23	124,793	NA	NA	4972	NA	28.4
Cincinnati-0048	OH	39-061-0048	10	152,115	360,578	320	26027	NA	3.5
Cleveland-0073	OH	39-035-0073	41	181,956	340,537	122	NA	NA	16.4
Columbus-0038	OH	39-049-0038	32	135,746	272,758	122	12127	NA	4.1
Denver-0027	CO	08-031-0027	13	254,000	268,401	60	23206	NA	0
Denver-0028	CO	08-031-0028	16	230,000	252,563	351	NA	NA	0
Detroit-0093	MI	26-163-0093	8	156,800	210,034	NA	8307	NA	0
Fort Lauderdale-0035	FL	12-011-0035	12	300,000	609,962	317	9786	NA	6.1
Fort Lee-0010	NJ	34-003-0010	22	282,912	556,501	353	24869	NA	7.6
Fort Worth-1053	TX	48-439-1053	38	159,040	209,139	112	NA	NA	0
Hartford-0025	CT	09-003-0025	21	164,300	238,235	118	26065	NA	0
Houston-1052	TX	48-201-1052	19	193,105	319,977	118	NA	NA	0
Indianapolis-0087	IN	18-097-0087	25	165,672	316,144	118	19920	NA	0
Jacksonville-0108	FL	12-031-0108	35	146,000	319,374	361	NA	NA	25.9
Kansas City-0042	MO	29-095-0042	34	119,477	362,706	357	24795	NA	0
Lakeville-0480	MN	27-037-0480	34	83,000	184,317	359	NA	NA	0

Site Name	State	AQS ID	Distance to Road (m)	AADT	FE-AADT	N $PM_{2.5}$ Days	N BC Hours	N UFP Hours	Distance to Meteorology Site (km)
Las Vegas-1501	NV	32-003-1501	18	297,000	404,177	340	NA	NA	0
Laurel-0006	MD	24-027-0006	17	199,131	482,296	359	15872	6124	0
Livonia-0095	MI	26-163-0095	56	193,400	313,407	122	3581	NA	13.3
Long Beach-4008	CA	06-037-4008	24	190,000	612,560	342	NA	NA	0
Louisville-0075	KY	21-111-0075	33	188,697	286,634	88	NA	NA	6.4
Memphis-0100	TN	47-157-0100	22	157,380	327,350	120	NA	NA	2.1
Milwaukee-0056	WI	55-079-0056	53	161,167	161,167	NA	16300	NA	0
Minneapolis-0962	MN	27-053-0962	35	250,000	349,504	362	14370	NA	0
Nashville-0040	TN	47-037-0040	28	156,920	368,762	341	NA	NA	5.3
New Orleans-0021	LA	22-071-0021	32	98,800	187,721	118	NA	NA	12.8
Oakland-0012	CA	06-001-0012	24	225,000	441,675	363	24019	NA	9.1
Oklahoma City-0097	OK	40-109-0097	20	165,000	207,768	275	14547	NA	0
Ontario-0027	CA	06-071-0027	18	217,000	631,557	354	NA	NA	0
Philadelphia-0075	PA	42-101-0075	14	118,498	244,832	351	NA	NA	10.7
Philadelphia-0076	PA	42-101-0076	25	210,456	344,929	349	NA	NA	10.8
Pleasanton-0015	CA	06-001-0015	15	233,000	NA	271	NA	NA	39.2
Portland-0005	OR	41-067-0005	24	162,700	301,466	121	8733	NA	30.1
Providence-0030	RI	44-007-0030	5	159,500	356,833	363	24307	8948	2.4
Queens-0125	NY	36-081-0125	29	170,874	330,810	115	NA	14692	0.5
Raleigh-0021	NC	37-183-0021	19	158,000	227,789	347	NA	NA	22.2
Richmond-0025	VA	51-760-0025	17	159,954	275,121	116	NA	NA	7.2
Rochester-0015	NY	36-055-0015	11	98,306	128,179	113	NA	20398	0.8
Sacramento-0015	CA	06-067-0015	23	190,800	487,258	116	21830	NA	0
San Antonio-1069	TX	48-029-1069	38	211,409	424,510	90	NA	NA	0
San Jose-0006	CA	06-085-0006	33	251,000	386,540	359	8027	NA	4.1
Seattle-0030	WA	53-033-0030	11	167,093	332,515	362	10370	NA	0
Springfield-0031	VA	51-059-0031	18	248,891	463,561	361	NA	NA	22.5
St. Louis-0094	MO	29-510-0094	21	147,943	334,351	364	25365	NA	0
St. Petersburg-0027	FL	12-103-0027	26	145,500	230,618	NA	21996	NA	8.9
Tacoma-0024	WA	53-053-0024	13	163,109	324,587	359	NA	NA	9.5
Tampa-0113	FL	12-057-0113	34	216,000	371,520	NA	17792	14875	23.6
Tempe-4019	AZ	04-013-4019	13	267,488	521,640	365	NA	NA	0
Washington DC-0051	DC	11-001-0051	15	130,892	195,802	355	NA	NA	0
Wilkinsburg-1376	PA	42-003-1376	23	74,421	126,040	365	NA	NA	8.8

2.1.2 Meteorological Data

For all near-road sites, the hourly wind direction data were used to characterize times when the near-road monitor was upwind or downwind of the road, or when winds were parallel to the road. First, the angle from the near-road monitor to the center of the nearby road was deduced from the coordinates using ArcMap. Then, the wind direction was classified as upwind, downwind, or parallel, using 120 degree bins for each category. The percentage of time for each wind category was calculated for each year. Hourly wind speed was used to calculate annual average wind speed. Meteorological variables were used to assess particulates based on their analysis period: the year 2018 for $PM_{2.5}$ and 2016-2018 for BC and UFP.

2.1.3 Land Use

In order to examine land use characteristics of the domains around the near-road sites, we used the NLCD developed by the USGS. The gridded data products of imperviousness and land cover from the most recently available NLCD (2011 at the time of this work), at 30-meter resolution, were used. Imperviousness is defined between 0 and 100%, with 100% representing impervious concrete, and 0% representing natural environments such as soil. The land use product contains 96 different categories. These categories were classified into three bins: urban, 50% urban, and non-urban. This process was carried out for near-road sites and nearby ambient sites. Based on these criteria, and on a visual examination identifying the densest urban regions, the commonality of land use between near-road and nearby ambient site was determined.

2.2 $PM_{2.5}$ Increment Calculation

The daily ambient $PM_{2.5}$ measurements within 40 km of each near-road site were used to estimate the background $PM_{2.5}$ concentrations. Background $PM_{2.5}$ was estimated at near-road sites using two methods: (1) using an inverse distance weighting (IDW) average of multiple monitors, and (2) using the nearest ambient monitor to represent background concentrations (nearest-monitor method). For the IDW method, ambient sites are given a relative weighting factor that is proportional to the inverse length of the distance from the near-road monitor squared, so that sites closer to the near-road monitor play a stronger role in representing the background. This method follows EPA guidance[1] and is consistent with the method employed by previous studies (Seagram et al., 2019b; Mukherjee et al., 2019). Daily $PM_{2.5}$ near-road increments were calculated in both the IDW and nearest-monitor methods as the difference between the near-road value and the background value. Daily $PM_{2.5}$ increments were then averaged up to an annual average $PM_{2.5}$ increment.

Increments were calculated only where there were identical sampling methods at near-road and nearby sites. After restricting for identical methods, 46 near-road sites were found to have at least

[1] See Section 8 in epa.gov/state-and-local-transportation/project-level-conformity-and-hot-spot-analyses#pmguidance.

one ambient site within 40 km that met completeness thresholds. Following the procedure from a previous study, the confounding factors of land use, proximity to sea breeze (within 5 km), and immediate near-road site factors were evaluated for each near-road site (Mukherjee et al., 2019). After removing near-road sites where any of these confounding factors was present, a final set of 32 near-road sites was chosen. We present increments for this final set of 32 near-road sites, categorized by their instrument method type: FRM or FEM.

Two sources of uncertainty were calculated for the annual average increment: the uncertainty due to instrument bias, and the statistical uncertainty on the mean. The average bias percentage by instrument type was found from the EPA quality assessment of 2011-2013 data (U.S. Environmental Protection Agency, 2015b). The daily uncertainty due to instrument bias was calculated by multiplying the bias percentage with the daily near-road and ambient measurement. The daily uncertainty of the increment was calculated as the root sum of squared (RSS) of uncertainties from near-road and ambient data. The annual average uncertainty due to instrument bias was found by taking an annual average of daily uncertainties. The statistical uncertainty is calculated as the 95% confidence interval on the mean, defined as

$$Statistical\ uncertainty\ =\ 1.96\ \times\ standard\ deviation(increment)\sqrt{(N-1)}$$

where N represents the valid number of days of data. The final uncertainty on the annual average increment is the RSS from the two sources: instrument bias and statistical uncertainty.

2.3 BC Increment Calculation

We calculated BC increments using two methods: (1) using an ambient nearby monitor (NM) to represent background BC and (2) using the time series method developed by Wang et al. (2018) to separate background and BC increment. For the nearby monitor method, hourly BC increments were calculated as the difference in the concentration between the near-road site and a representative ambient site. Typically, the closest ambient monitor with complete BC data was used. In some cases, the closest monitor was near a potential BC emission source, so another nearby monitor was selected. All 29 near-road sites for which BC data were available had a nearby monitor within 40 km that could be used to calculate a daily BC increment. Hourly increments from the 2016-2018 period were averaged up to annual and three-year average increments. The Wang et al. time series method separates out the “background” of a time series from the hourly fluxuations, providing an hourly estimate of “local” and “background” contributions. It does so by identifying the slower-varying, lower-frequency signals of urban- or regional-scale pollution from the local sources that have faster-varying, higher-frequency signals (Wang et al., 2018; Hilker et al., 2019). Details of the calculations can be found in Wang et al., 2018.

2.4 Comparison of Ambient Data with Site Characteristics

We use statistical measures to examine and quantify the relationship between particulates (incremental $PM_{2.5}$, total and incremental BC) and the following near-road site characteristics:

- The monitor's distance to the road
- AADT
- FE-AADT
- Average wind speed
- The percent of time the monitor was upwind, downwind, or parallel of the target roadway

The pairwise coefficient of determination (R^2) is computed to quantify the correlation: an R^2 value of 1 would correspond to perfect 1-to-1 correlation, and an R^2 value of 0 would correspond to no correlation. Regressions are used to examine the relationship between near-road concentrations and site characteristics, and the p-values of these regressions are used to see if the relationship is statistically significant. A p-value less than 0.05 would signify a statistically significant relationship with greater than 95% confidence.

3. Results

3.1 2018 $PM_{2.5}$ NAAQS Comparison for 52 Near-Road Sites

The distributions of daily average near-road $PM_{2.5}$ in 2018 from the 52 near-road sites are shown in **Figure 1**. The annual and 98th percentile daily average NAAQS for $PM_{2.5}$ are also shown. Figure 1 compares measured concentrations to the NAAQS for research purposes only and does not represent a calculation to determine attainment status. Six sites exceeded the annual average NAAQS of 12 µg/m^3: Ontario-0027, Oakland-0012, Pleasanton-0015, Long Beach-4008, Cincinnati-0048, and San Jose-0006. Five sites exceeded the daily 98th percentile $PM_{2.5}$ value of 35 µg/m^3: Oakland-0012, Pleasanton-0015, Berkeley-0013, San Jose-0006, and Long Beach-4008. The California Bay Area sites (Oakland-0012, Pleasanton-0015, San Jose-0006, Sacramento-0015, and Berkeley-0013) were impacted by the Camp Fire for over two weeks in 2018, resulting in higher-than-typical daily average $PM_{2.5}$. The Seattle-0030 and Tacoma-0024 sites were also impacted by wildfire smoke in 2018. Other non-traffic processes may also contribute to the $PM_{2.5}$ concentrations shown in Figure 1.

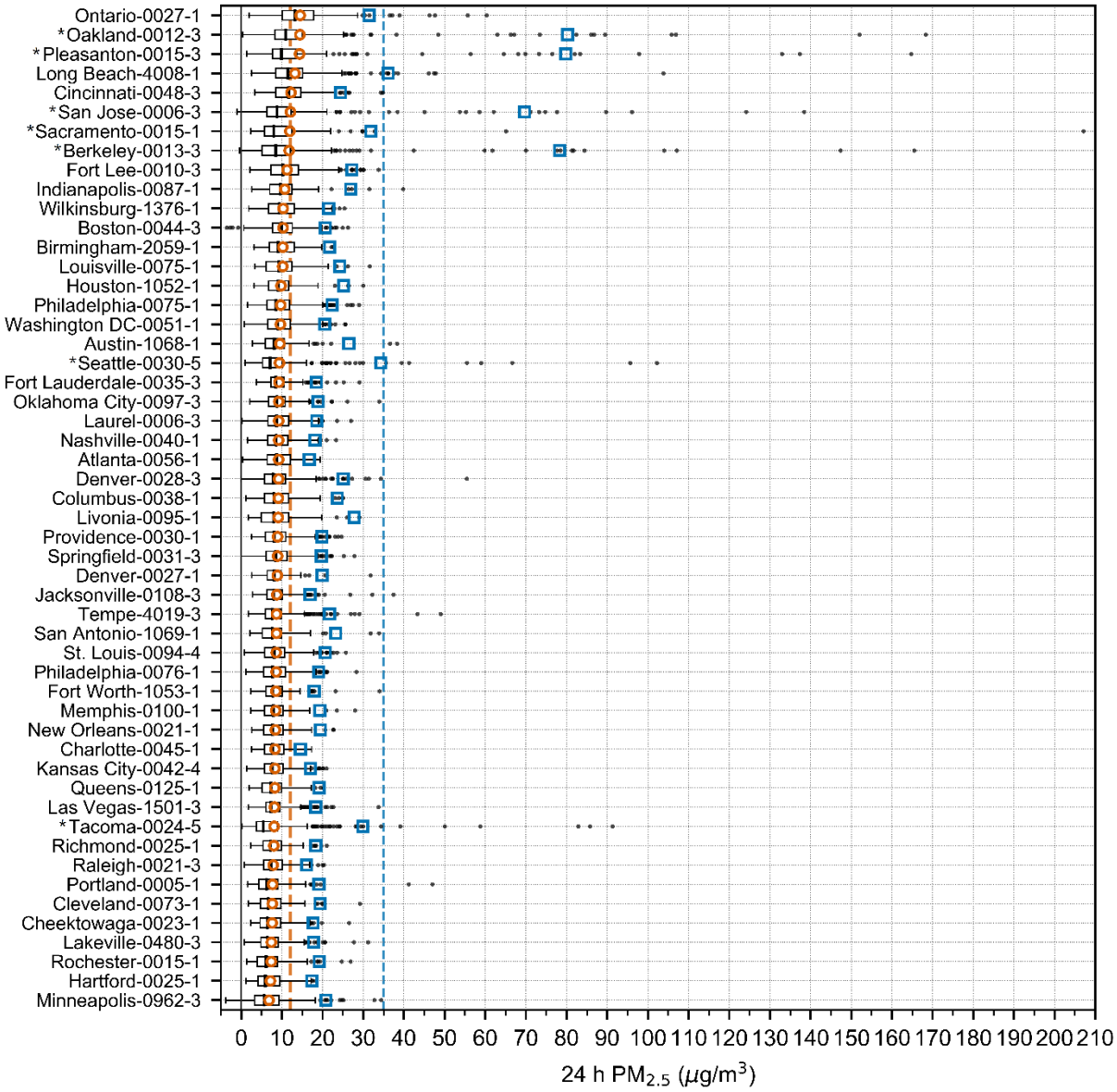

*$PM_{2.5}$ values from these sites were likely impacted by wildfires during November 8-21, 2018, in California and August 14-25, 2018, in Washington.

Figure 1. Distribution of daily average $PM_{2.5}$ at 52 near-road monitoring sites in 2018, sorted by annual mean. The annual mean (orange circles) and 98th percentile of 24 hr $PM_{2.5}$ concentrations (blue squares) are shown. The orange dashed lined denotes the annual NAAQS threshold (12 μg/m^3), and the blue dashed line denotes the daily average NAAQS threshold (35 μg/m^3).

3.2 2016-2018 $PM_{2.5}$ NAAQS Comparison for 26 Near-Road Sites

Of the 52 near-road sites shown in Figure 1, daily average $PM_{2.5}$ data for 26 sites met completeness thresholds for the years 2016, 2017, and 2018. The distributions of daily average $PM_{2.5}$ from those 26 sites are shown in Figure 2. Figure 2 compares measured concentrations to the NAAQS for research purposes only and does not represent a calculation to determine attainment status. Two sites, Ontario-0027 and Long Beach-4008, both in the Los Angeles area, exceeded the three-year annual average NAAQS of 12 µg/m^3. Three sites, Oakland-0012, San Jose-0006, and Ontario-0027, exceeded the three-year average daily 98th percentile $PM_{2.5}$ value of 35 µg/m^3. However, the California Bay Area sites Oakland-0012 and San Jose-0006 were impacted by the Camp Fire, which contributed to their high daily 98th percentile $PM_{2.5}$ values.

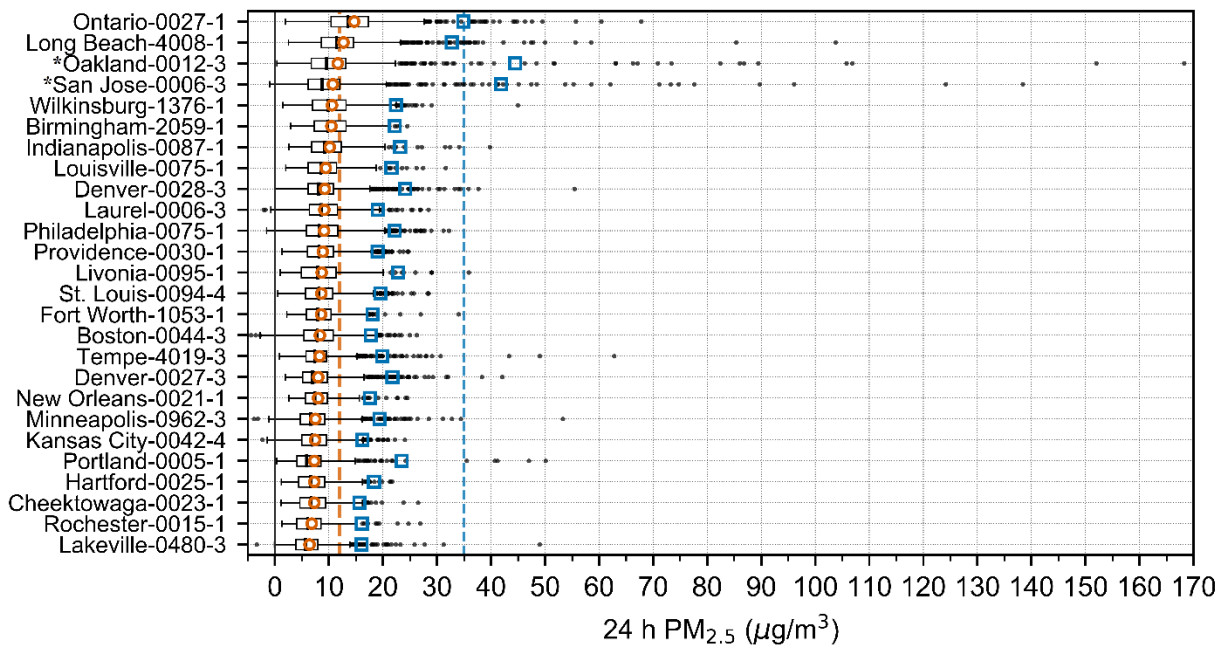

*$PM_{2.5}$ values from these sites were likely impacted by the Northern California Camp Fire, which occurred November 8-21, 2018.

Figure 2. Distribution of daily average $PM_{2.5}$ at 26 near-road monitoring sites from 2016 to 2018, sorted by three-year average annual mean. The three-year average annual mean (orange circles) and 98th percentile of 24 hr $PM_{2.5}$ concentrations (blue squares) are shown. The orange dashed lined denotes the annual NAAQS threshold (12 µg/m^3), and the blue dashed line denotes the daily average NAAQS threshold (35 µg/m^3).

3.3 Three-Year and Five-Year Annual Average $PM_{2.5}$ Trends at Near-Road Sites

We assessed trends for the near-road sites whose available data met completeness criteria for the five-year or three-year trend periods. Available data for seven near-road sites met completeness thresholds to calculate the five-year trend for 2014-2018; available data for 26 near-road sites met completeness thresholds to calculate the three-year trend for 2016-2018. The annual average $PM_{2.5}$ levels for each year and the associated trend for each site is shown in **Figure 3**. The five-year trends of annual average $PM_{2.5}$ at the seven near-road sites show a decreasing trend in annual average $PM_{2.5}$ levels for most sites, with the notable exception of Kansas City-0042. The three-year trends of annual average $PM_{2.5}$ at 26 near-road sites do not display a consistent overall pattern. These 26 sites were categorized based on their trend into: nine sites with a negative trend (negative slope of regression), nine sites with a low positive trend (trend between 0 and 0.5 $\mu g/m^3$ per year), and eight sites with a high positive trend (trend greater than 0.5 $\mu g/m^3$ per year). Oakland-0012 and San Jose-0006 were influenced by wildfires in 2018 as previously discussed. The annual average $PM_{2.5}$ values for 2016-2018, and the three-year trends are presented in the Appendix.

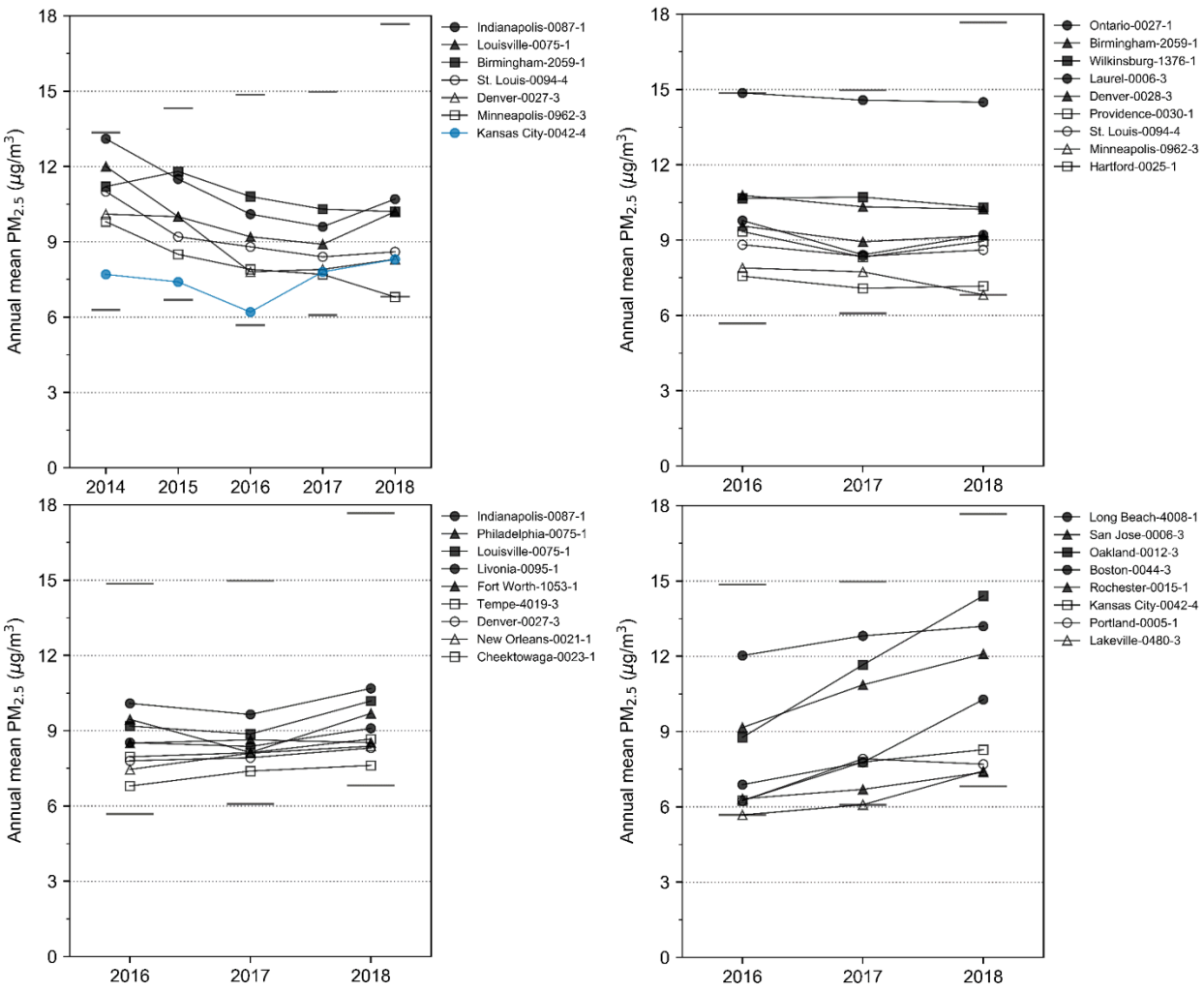

Figure 3. Distribution and trends of annual average $PM_{2.5}$ at near-road monitoring sites. Top left: five-year trend from 2014-2018 for the 7 near-road sites that met completeness thresholds for each year. Three-year trends from 2016-2018 are presented for the 26 near-road sites that met completeness thresholds for each year. Top right: 9 sites with a negative trend. Bottom left: 9 sites with a low positive trend. Bottom right: 8 sites with a high positive trend. Horizontal bars signify the highest and lowest annual average from all near-road sites for that year.

3.4 $PM_{2.5}$ Increments at Near-Road Sites Before Removal of Sites Affected by Confounding Factors

The range of annual average $PM_{2.5}$ increment values calculated using the IDW method and the nearest-monitor method to represent background concentrations is shown in **Figure 4**. Only the 46 sites with identical instrument comparisons are shown; of these sites, 34 sites had only positive increments and 12 sites had a negative increment using the IDW method, the nearest-monitor method, or both. A negative increment indicates that the $PM_{2.5}$ value from the urban background estimate was higher than the value from the near-road site; while this is not a physically meaningful result, it does help to provide an indication of the uncertainty associated with characterizing urban background $PM_{2.5}$ concentrations representing the upwind concentrations at near-road sites.

Two sites, Fort Lauderdale-0035 (2.82 ± 3.21 μg/m^3) and Laurel-0006 (2.49 ± 1.42 μg/m^3), had IDW increments greater than 2.0 μg/m^3. IDW increments were between 1 and 2 μg/m^3 for 13 near-road sites, between 0.5 and 1 μg/m^3 for 10 sites, and between 0 and 0.5 μg/m^3 for 11 sites. The distribution of IDW and nearest-monitor increments is very similar. The uncertainty of each annual average increment and the instrument method type, FEM or FRM, is shown in Figure 4. FEM instruments resulted in higher measurement bias uncertainty. The four near-road sites with the highest increments all used FEM instruments. Of the 12 near-road sites with a negative increment, 9 sites used FEM instruments.

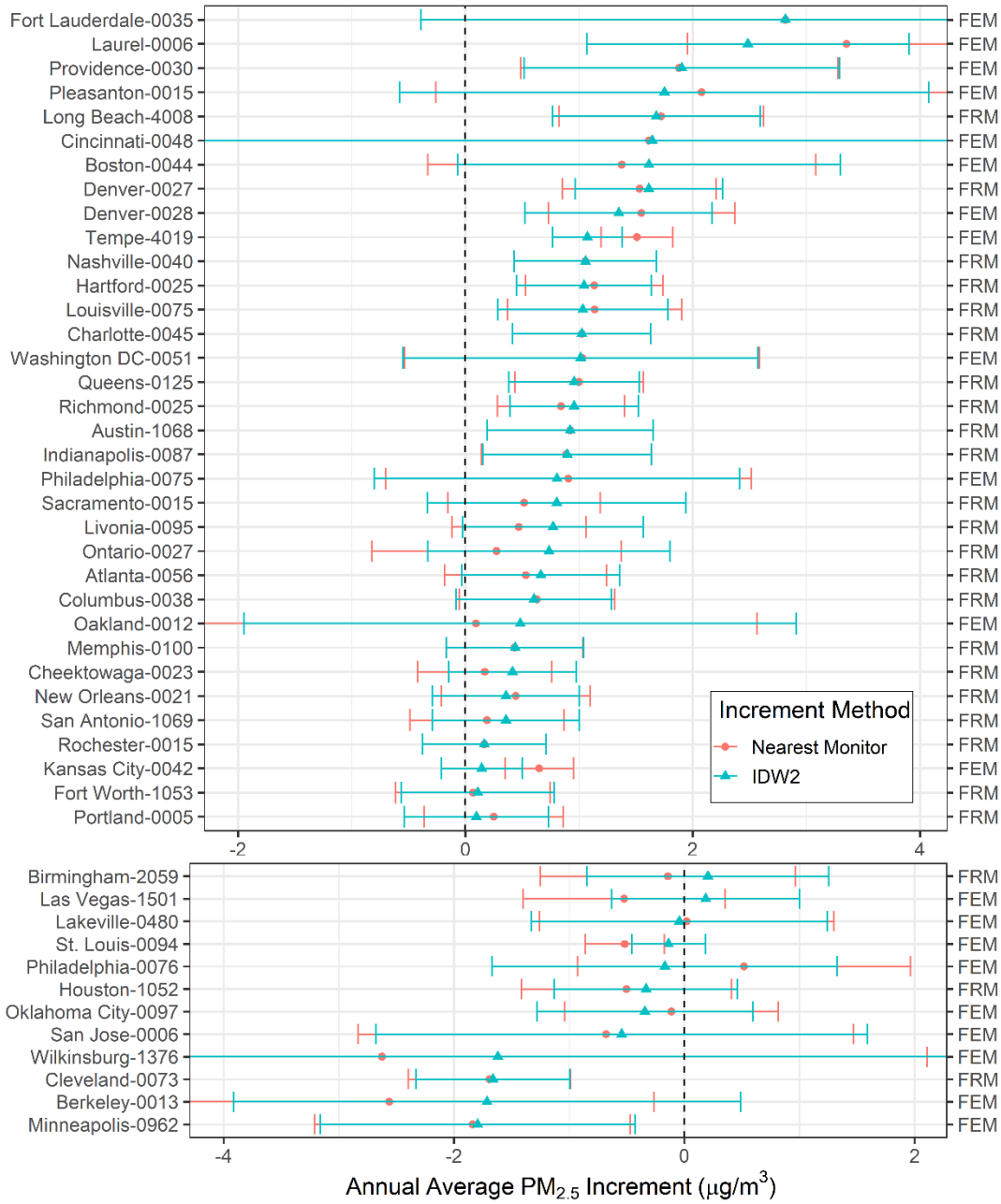

Figure 4. Distributions of annual average $PM_{2.5}$ increments using identical instrument methods from 46 near-road sites, computed using IDW and the nearest-monitor method. The 34 near-road sites with all positive increments are shown at the top, and the 12 near-road sites with any negative increments are shown at the bottom. The instrument measurement type (FRM vs. FEM) is shown for each site. Uncertainty bars represent instrument bias and statistical uncertainty of the mean. The full uncertainty bars are shown in Appendix Figure A-5.

3.5 $PM_{2.5}$ Increments at 32 Sites After Removal of Sites Affected by Confounding Factors

After removing sites with a confounding factor—the immediate site environment, land use, and proximity to sea breeze (as described in Section 2.2)—a final list of 32 sites, a subset of the 46 sites above, was determined. Table 2 lists the 32 sites, increments, increment uncertainties, and site characteristics. Increments are presented only where identical methods were available at the near-road and nearby sites.

Of these 32 sites, 19 sites had a FRM instrument and 13 sites had a FEM instrument to calculate the increment; the FRM and FEM sites are plotted separately in Figure 5. The FRM sites have less increment uncertainty, as well as a smaller difference between their IDW and nearest-monitor increments. The FRM increments range from near-zero to 1.68 ± 0.91 μg/m^3 (observed at Long Beach-4008). The FRM increments from 7 sites range from near-zero to 0.5 μg/m^3 and for the other 12 sites range from 0.5 to 1.68 μg/m^3. Among the FEM near-road sites, Laurel-0006, with an IDW increment of 2.49 ± 1.42 μg/m^3, had the only increment greater than 2.0 μg/m^3. The increments for 7 FEM sites were between 1 and 2 μg/m^3. The IDW increments for 4 FEM sites were negative; three of these increments range from -0.54 to -0.04 μg/m^3 and Minneapolis-0962 had a negative increment of -1.8 ± 1.37 μg/m^3. The negative increment at Minneapolis-0962 indicates that the urban background concentrations were higher than the near-road site; we did not identify any confounding factor for this near-road site. The range of positive IDW increments shown in Figure 5 corresponds to a contribution between 1% and 27% from roadways to annual average $PM_{2.5}$, as shown in Table 2. These contributions are comparable to the results of Dabek-Zlotorzynska et al. (2019) which found that on-road emissions contributed between 15% and 35% of near-road $PM_{2.5}$ at 3 sites stationed between 6 and 15 meters from the roadway in Canada. When we restrict the results in Table 2 for the 9 sites 15 meters or less than the roadway, we find roadway contributions range from 2% to 21%.

Table 2. Near-road site characteristics, 2018 increments, and increment uncertainties from the IDW and nearest-monitor methods for the 32 near-road sites. Table is rank-ordered by IDW $PM_{2.5}$ increment. Roadway contribution is calculated as the IDW $PM_{2.5}$ increment percentage of total annual average $PM_{2.5}$, for sites with a positive increment.

Site Name	AQS ID	Annual Average $PM_{2.5}$ ($\mu g/m^3$)	N Days Increment Data	IDW $PM_{2.5}$ Increment ($\mu g/m^3$)	IDW $PM_{2.5}$ Increment Uncertainty ($\mu g/m^3$)	N of Background Stations (IDW)	Roadway Contribution (%)	Nearest Monitor $PM_{2.5}$ Increment ($\mu g/m^3$)	Nearest Monitor $PM_{2.5}$ Increment Uncertainty ($\mu g/m^3$)	Distance to Road (meters)	AADT	FE-AADT	Method Type
Laurel-0006	24-027-0006	9.2	345	2.49	1.42	4	27.1	3.35	1.4	17	199,131	482,296	FEM
Providence-0030	44-007-0030	8.95	353	1.91	1.39	5	21.3	1.88	1.4	5	159,500	356,833	FEM
Pleasanton-0015	06-001-0015	14.32	269	1.75	2.33	6	12.2	2.08	2.34	15	233,000	NA	FEM
Long Beach-4008	06-037-4008	13.2	327	1.68	0.91	2	12.7	1.72	0.9	24	190,000	612,560	FRM
Cincinnati-0048	39-061-0048	12.22	319	1.64	5.53	2	13.4	1.62	5.54	10	152,115	360,578	FEM
Denver-0027	08-031-0027	8.86	58	1.61	0.65	6	18.2	1.53	0.68	13	254,000	268,401	FRM
Boston-0044	25-025-0044	10.27	329	1.61	1.68	3	15.7	1.38	1.71	10	205,861	261,441	FEM
Denver-0028	08-031-0028	9.18	338	1.35	0.82	3	14.7	1.55	0.82	16	230,000	252,563	FEM
Tempe-4019	04-013-4019	8.67	365	1.07	0.31	7	12.3	1.51	0.31	13	267,488	521,640	FEM
Hartford-0025	09-003-0025	7.16	54	1.04	0.59	2	14.5	1.14	0.61	21	164,300	238,235	FRM
Louisville-0075	21-111-0075	10.18	88	1.03	0.75	4	10.1	1.14	0.77	33	188,697	286,634	FRM
Charlotte-0045	37-119-0045	8.31	56	1.03	0.61	1	12.4	1.03	0.61	36	154,000	262,535	FRM
Washington DC-0051	11-001-0051	9.6	351	1.01	1.56	2	10.5	1.03	1.56	15	130,892	195,802	FEM
Queens-0125	36-081-0125	8.25	107	0.96	0.57	15	11.6	1	0.57	29	170,874	330,810	FRM
Richmond-0025	51-760-0025	8	109	0.96	0.57	4	12	0.84	0.56	17	159,954	275,121	FRM
Austin-1068	48-453-1068	9.51	39	0.92	0.73	1	9.7	0.92	0.73	43	144,013	268,441	FRM
Indianapolis-0087	18-097-0087	10.68	111	0.9	0.74	6	8.4	0.89	0.75	25	165,672	316,144	FRM
Sacramento-0015	06-067-0015	11.95	91	0.8	1.14	3	6.7	0.52	0.67	23	190,800	487,258	FRM
Atlanta-0056	13-121-0056	9.19	119	0.66	0.7	5	7.2	0.53	0.71	7	382,000	544,678	FRM
Columbus-0038	39-049-0038	9.11	121	0.6	0.69	2	6.6	0.63	0.68	32	135,746	272,758	FRM
Memphis-0100	47-157-0100	8.48	116	0.44	0.6	3	5.2	0.43	0.6	22	157,380	327,350	FRM

Site Name	AQS ID	Annual Average $PM_{2.5}$ ($\mu g/m^3$)	N Days Increment Data	IDW $PM_{2.5}$ Increment ($\mu g/m^3$)	IDW $PM_{2.5}$ Increment Uncertainty ($\mu g/m^3$)	N of Background Stations (IDW)	Roadway Contribution (%)	Nearest Monitor $PM_{2.5}$ Increment ($\mu g/m^3$)	Nearest Monitor $PM_{2.5}$ Increment Uncertainty ($\mu g/m^3$)	Distance to Road (meters)	AADT	FE-AADT	Method Type
Cheektowaga-0023	36-029-0023	7.61	112	0.41	0.56	2	5.4	0.17	0.59	20	126,107	212,275	FRM
New Orleans-0021	22-071-0021	8.38	106	0.36	0.65	3	4.3	0.44	0.65	32	98,800	187,721	FRM
San Antonio-1069	48-029-1069	8.66	46	0.36	0.65	2	4.2	0.19	0.68	38	211,409	424,510	FRM
Birmingham-2059	01-073-2059	10.22	60	0.2	1.05	4	2	-0.14	1.11	25	126,670	193,362	FRM
Las Vegas-1501	32-003-1501	8.16	333	0.19	0.82	5	2.3	-0.52	0.88	18	297,000	404,177	FEM
Rochester-0015	36-055-0015	7.37	100	0.17	0.54	1	2.3	0.17	0.54	11	98,306	128,179	FRM
Fort Worth-1053	48-439-1053	8.52	103	0.11	0.67	2	1.3	0.07	0.68	38	159,040	209,139	FRM
Lakeville-0480	27-037-0480	7.43	356	-0.04	1.29	3	NA	0.02	1.28	34	83,000	184,317	FEM
Philadelphia-0076	42-101-0076	8.59	340	-0.17	1.5	3	NA	0.52	1.45	25	210,456	344,929	FEM
San Jose-0006	06-085-0006	12.09	356	-0.54	2.13	4	NA	-0.68	2.15	33	251,000	386,540	FEM
Minneapolis-0962	27-053-0962	6.82	359	-1.8	1.37	6	NA	-1.84	1.37	35	250,000	349,504	FEM

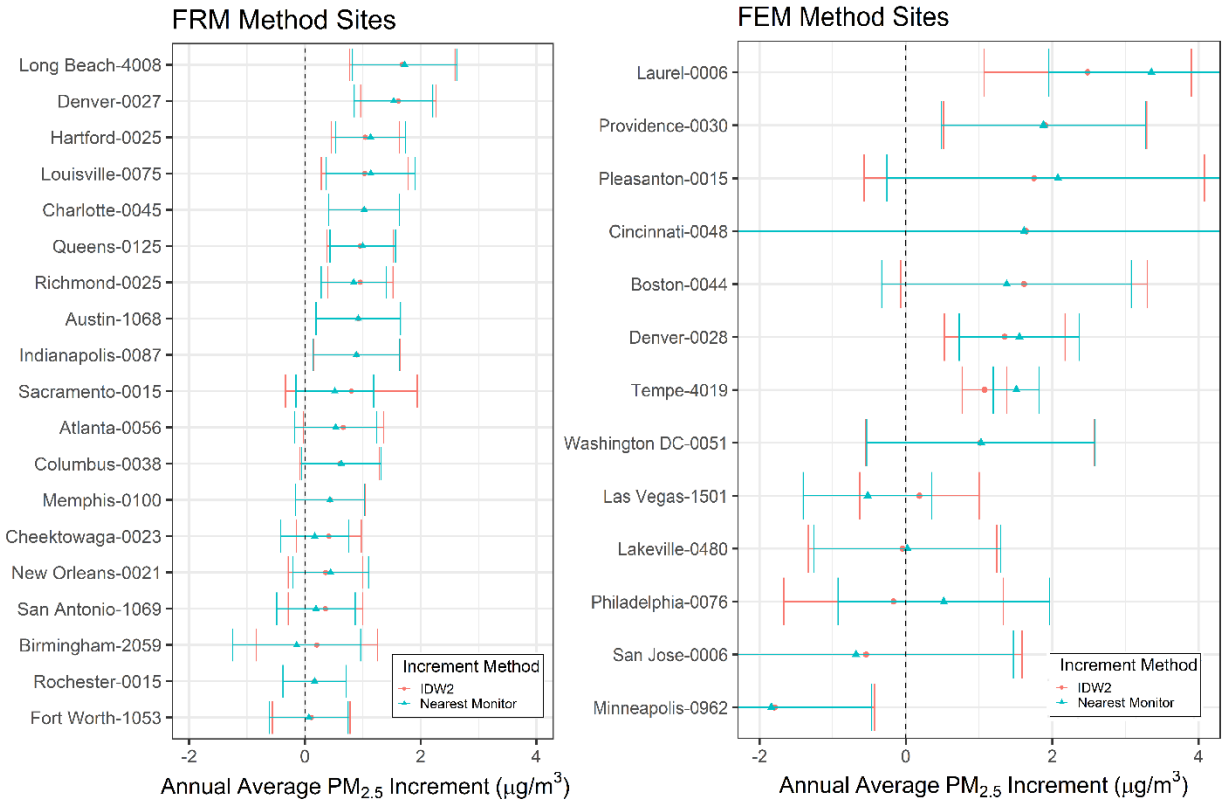

Figure 5. Distributions of 2018 annual average $PM_{2.5}$ increments computed using IDW and nearest-monitor calculation. Increments are shown for the 32 near-road sites that remained after all sites with a noted confounding factor were removed. Left: Data from 19 near-road sites calculated with an FRM instrument. Right: Data from 13 near-road sites calculated from FEM instruments. The full uncertainty bars are presented in the Appendix.

Figure 6 shows the same annual average increments shown in Figure 5, aggregated through boxplots. The plots show more clearly that the FEM sites have a greater range and variability than the FRM sites. The full range of the FEM sites (represented by line segments in the boxplot) are largely driven by the Laurel-0006 and Minneapolis-0962 sites. Excluding those sites would lead to an FEM increment range from -0.54 μg/m^3 to 1.91 μg/m^3. The inter-quantile range (IQR) of the FEM increments is very similar to the whole range of the FRM increments, going from near-zero to about 1.7 μg/m^3. The IQR of the FRM increments goes from approximately 0.5 μg/m^3 to approximately 1.1 μg/m^3. Very similar distributions are seen between IDW and nearest-monitor increments for both FEM and FRM instruments.

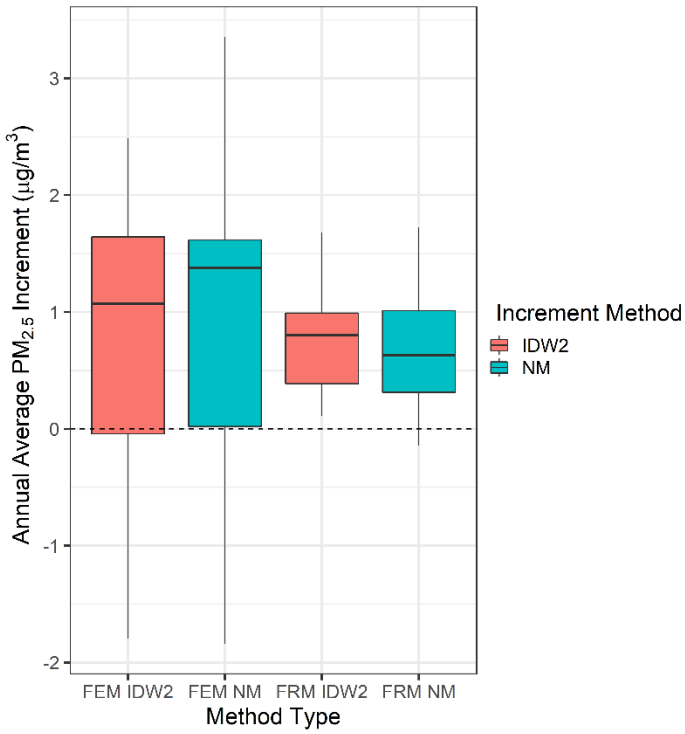

Figure 6. Boxplot distributions of 2018 annual average $PM_{2.5}$ increments computed using IDW and nearest-monitor calculation (NM). Increments are shown for the 32 near-road sites that remained after all sites with a noted confounding factor were removed. The box cutoffs are the inter-quantile ranges (IQRs), and the line segments show the full range.

3.6 Increment Comparison to Site Characteristic Variables

For the set of increments presented in Table 2, where all sites with a confounding factor have been removed, increments were compared to meteorology, traffic, and site characteristic variables using pairwise R^2 values and regressions. An R^2 value of 1 corresponds to perfect correlation, and an R^2 value of 0 would correspond to no correlation. These comparisons show which site characteristics are the most correlated with annual average incremental $PM_{2.5}$ values. Only positive increments were used in these comparisons. Table 3 shows the R^2 values between IDW and nearest-monitor increments for the following variables: the monitor distance to the target road; FE-AADT; AADT; percentage of time the monitor was upwind, downwind or parallel; and average wind speed. The monitor distance to road was the most strongly correlated with the 2018 increments for both IDW and nearest-monitor methods, with an R^2 value of 0.18 and 0.19, respectively. FE-AADT, percentage of time upwind, and AADT also show some correlations (R^2 values ranging from 0.03 to 0.14 for the nearest-monitor method and from 0.09 to 0.17 for the IDW method). Average wind speed and percentage of time parallel or downwind show no correlation.

Table 3. Coefficient of determination (R^2 value) for IDW and nearest-monitor increments with near-road site and meteorological variables for 2018. The comparisons are shown for increments from Table 2, after removing sites with confounding factors. Only positive increments were used for pairwise R^2 values. Variables are rank-ordered by R^2 values.

Variable	IDW Method	Nearest Monitor
Distance to Road	0.18	0.19
FE-AADT	0.14	0.17
Percent Upwind	0.05	0.14
AADT	0.03	0.09
Average Wind Speed	0.03	0.07
Percent Parallel	0.03	0.01
Percent Downwind	0.01	0.01

Regressions shown in Figure 7 were calculated to compare the IDW increment with the four variables that showed the highest R^2 correlation: the monitor distance to road, FE-AADT, percentage of time upwind, and AADT. A linear regression ($y = a \cdot x + b$) was used for FE-AADT, percentage of time upwind, and AADT, and an inverse relationship ($y = a /x + b$) was used for distance to road. The coefficients and p-values of these regressions are shown in Table 4. The p-values show that the modeled relationships are statistically significant at a 95% confidence level for the variables FE-AADT and monitor distance to road (p-values less than or equal to 0.05). A stronger statistical relationship to the increment is seen with FE-AADT than with AADT (both higher R^2 and lower p-value), showing the importance of heavy duty vehicles on incremental $PM_{2.5}$. The regression for distance to road predicts an increment of 2 μg/m^3 at 5 m from the roadway falling to approximately 1 μg/m^3 at 15 m from the roadway (96% confidence that the relationship exists). The linear regression for FE-AADT predicts a relationship of 0.18 μg/m^3 higher $PM_{2.5}$ values for every increase of 100,000 in FE-AADT (95% confidence).

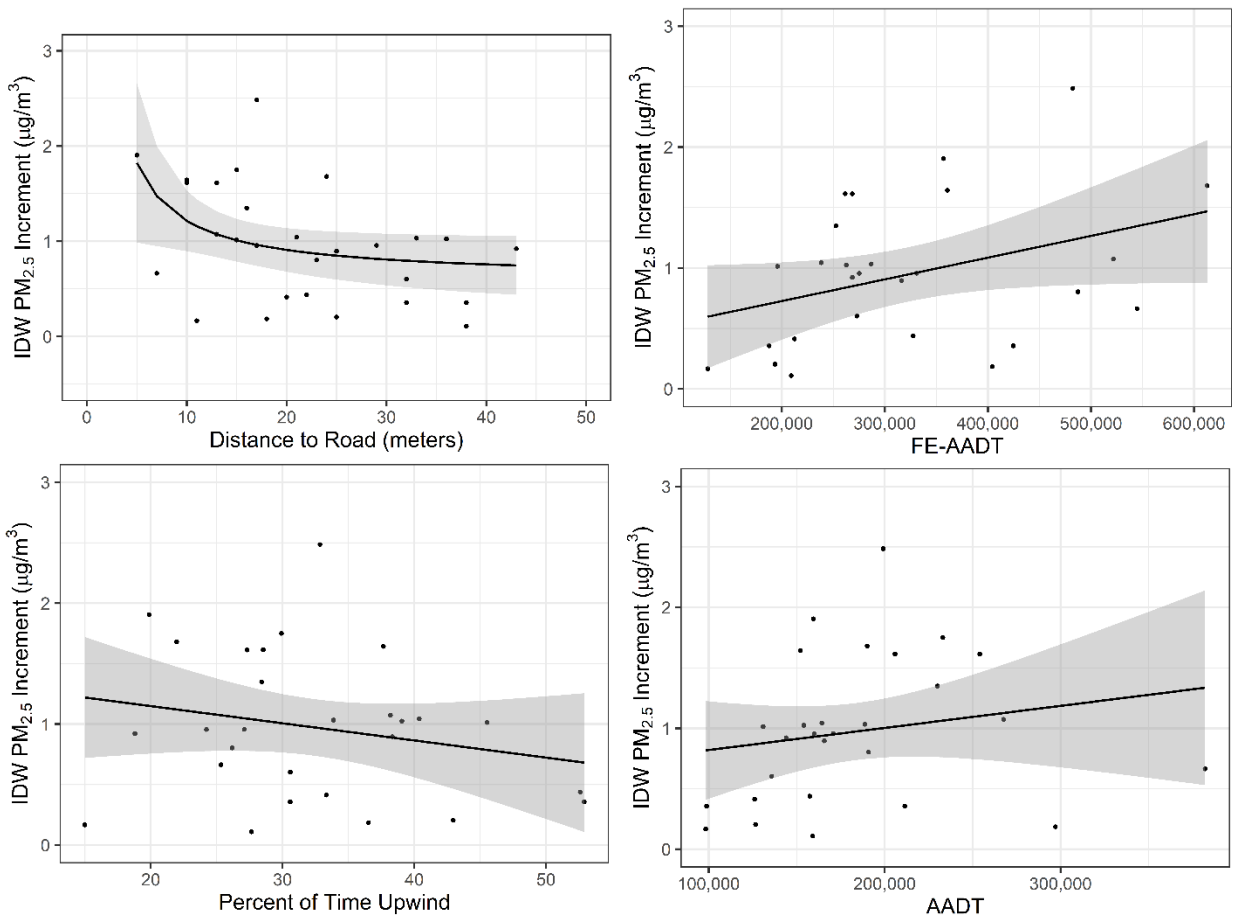

Figure 7. The relationship between the 2018 IDW $PM_{2.5}$ increment in comparison to distance to road (upper left), FE-AADT (upper right), percentage of time upwind of the roadway (lower left), and AADT (lower right). Regressions are shown in black, with the range of the standard error of the regression line shown in dark gray.

Table 4. The intercepts, slopes, p-values, and R^2 values for the four regressions presented in Figure 7. For FE-AADT, AADT and percent upwind a linear regression is used, of the form $y = a \cdot x + b$. For distance to road, an inverse relationship is used, of the form $y = a/x + b$.

Regression Model	Distance to Road vs. IDW Increment	FE-AADT vs. IDW Increment	Percent Upwind vs. IDW Increment	AADT vs. Increment
a	6.08	$1.80 \cdot 10^{-6}$	-0.014	$1.83 \cdot 10^{-6}$
b	0.60	0.37	1.43	0.64
p-value	0.04*	0.05*	0.26	0.34
R^2	0.18	0.14	0.05	0.03

*Showing a greater than 95% statistical significance

3.7 Comparing 2018 and 2017 $PM_{2.5}$ Increments

A previous study examined near-road annual average $PM_{2.5}$ increments from 2017 (Mukherjee et al. 2019). That study used the same methodology to calculate nearest monitor and IDW increments, presented for a final set of 20 sites, after removing for the same confounding factors as this study, and restricting for identical instrument comparisons. Increments from those 20 sites ranged from 0.13 µg/m^3 at Minneapolis-0962 to 2.04 µg/m^3 at Providence-0030 in 2017. Laurel-0006 had increment values of IDW: 0.99 µg/m^3 and nearest monitor: 1.13 µg/m^3. The previous study presented implications for determining transportation projects of local air quality concern (POAQC) based on 2017 increments from those 20 sites.

The current study used the same methodology for calculating nearest monitor and IDW increments for 2018, which were presented for a final set of 32 sites, after removing for confounding factors and restricting for identical instrument comparisons. Due to differences in data completeness, increments based on 2018 data may be calculated from a different set of ambient monitors for a given near-road site. The current (2018 data) study presents a more detailed calculation of uncertainty on the increment, which includes the instrument bias for FRM or FEM instruments and statistical uncertainty. Uncertainty for 2017 increments was calculated only based on statistical uncertainty.

While the 20 sites from 2017 included no negative increments, in 2018 six of the 32 sites have a negative increment (nearest monitor, IDW or both). Five of these six sites with a negative increment were based on FEM instruments. The lowest 2018 increment was Minneapolis-0962 (IDW: -1.8 ± 1.37 µg/m^3, nearest monitor: -1.84 ± 1.37 µg/m^3). The highest 2018 increment was at Laurel-0006 (IDW: 2.49 ± 1.42 µg/m^3, nearest monitor: 3.35 ± 1.4 µg/m^3). The second highest 2018 increment was at Pleasanton-0015 (IDW: 1.75 ± 2.33 µg/m^3, nearest monitor: 2.08 ± 2.34 µg/m^3). Laurel-0006 and Pleasanton-0015 were the only sites with an increment greater than 2.04 µg/m^3, the maximum increment calculated from 2017 data in the previous work. Laurel-0006, Providence-0030 and Pleasanton-0015 were the only sites with an increment greater than 1.72 µg/m^3. All three of these sites were based on FEM instruments. We show that FEM-based increments almost always have higher uncertainty than FRM-based increments, due to inherent instrument bias (as shown in Figure 4 and Table 2).

We examined the case of Laurel-0006 in greater detail, to better understand its relatively high 2018 increment value. Laurel-0006 has only an FEM instrument available. The increment value from Laurel-0006 is primarily determined by its nearest ambient monitoring station, 24-033-0030, 10 km away. EPA presents a comparability assessment of ambient monitors where collocated instruments are available (https://www.epa.gov/outdoor-air-quality-data/pm25-continuous-monitor-comparability-assessments). The ambient site, 24-033-0030, had one FEM instrument and two collocated FRM instruments. The FEM instrument reads low relative to the two FRM instruments, with slopes of regression of 0.90 and 0.71. Correcting the FEM instrument to its collocated FRM instruments would change the resulting increments, leading to lower increment values at Laurel-0006 of approximately

0.6 µg/m^3 or 1.7 µg/m^3. This confirms the higher uncertainty we present on the 2018 Laurel-0006 increment (±1.4 µg/m^3) due to its FEM instrumental uncertainty.

The overall distribution of our 2018 increments (see Figures 5 and 6, and discussion in section 3.5) is very similar to the distribution presented for 2017 increments. While it may be possible that the near-road incremental impact at Laurel-0006 is higher than 2.0 µg/m^3, the uncertainty for any given FEM-based increment is high relative to its magnitude. After examining the whole distribution of 2018 increments, the range of 2018 FRM increments (-0.14 ± 1.11 µg/m^3 to 1.68 ± 0.91 µg/m^3 from 19 sites) and noting the specific irregularities of the nearby ambient monitor at Laurel-0006, we conclude that the results we presented in 2017 and implications for POAQC determination are still consistent with the 2018 results.

3.8 Near-Road Ultrafine Particle Concentrations

UFP measurements from the years 2016-2018 were available at six near-road monitoring sites: Tampa-0113, Cheektowaga-0023, Rochester-0015, Queens-0125, Providence-0030, and Laurel-0006. Average concentrations ranged from a high of 5.1 x 10^4 particles/cm^3 at Providence-0030, which is the site closest to the adjacent freeway at 5 m, to a low of 1.3 x 10^4 particles/cm^3 at Rochester-0015, which is the site with the lowest AADT (98,306 vehicles/day) and FE-AADT (128,179 vehicles/day). This average is typical of roadside concentrations, which are historically between 3 x 10^4 and 5 x 10^4 particles/cm^3 (Health Effects Institute, 2013; Morawska et al., 2008). Complete years of UFP data were not available at any nearby sites, so increments were not calculated.

UFP concentrations peaked in the morning at each site, between 0500 and 0700 local time, typical of near-road and urban locations. Providence-0030, Tampa-0113, and Laurel-0006 all showed small evening peaks as well, likely because these three sites had the highest traffic volume among the sites with UFP data. Concentrations were statistically significantly higher on weekdays compared to weekends at all sites, with the largest differences at Providence and Laurel (the sites with the highest FE-AADT), likely due to large changes in traffic volume between weekdays and weekends. The distribution of UFP concentrations by hour of day and by weekday versus weekend are shown in the Appendix.

When a near-road site was downwind of the adjacent freeway, UFP concentrations were statistically significantly higher than when the site was upwind of the freeway or when the winds were parallel to the freeway, with the exception of Rochester-0015 (see **Figure 8**). Median UFP concentrations were 1.4 to 3.5 times higher under downwind conditions, compared to upwind conditions. The differential between upwind and downwind conditions was lowest at the sites with the lowest FE-AADT (Cheektowaga-0023, Rochester-0015) and highest at the site with the highest FE-AADT (Laurel-0006, 482,296 vehicles per day). At the other three sites, FE-AADT was from of 330,000 to 370,000 vehicles per day, and downwind concentrations were 1.7 to 2.0 times higher than upwind concentrations. Overall, the trend of higher concentrations when a site is downwind of a freeway is likely more

impacted by FE-AADT than by distance, at least within the 5-34 m distance range of these near-road sites.

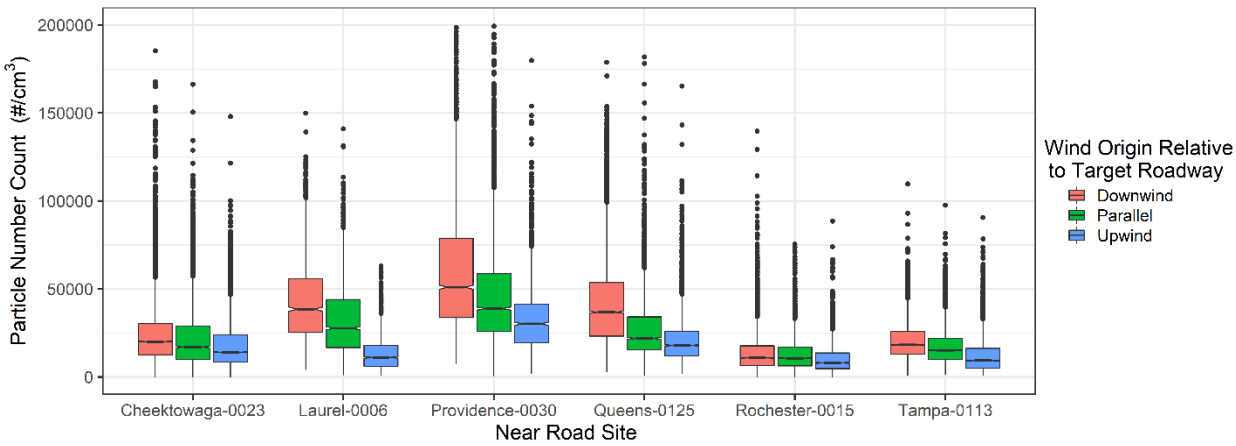

Figure 8. Box plot of 2016-2018 UFP concentrations by site under downwind, parallel, and upwind wind conditions.

3.9 Near-Road Black Carbon Concentrations

3.9.1 Black Carbon Concentration Distributions

BC concentrations from the years 2016-2018 were available for 29 sites representing a diverse set of traffic and meteorological conditions. For these 29 sites, AADT ranged from 119,477 to 382,000, FE-AADT ranged from 161,167 to 609,962, and the monitor distance to road ranged from 5 to 56 meters. Three-year average concentrations ranged from 0.62 µg/m^3 at St. Petersburg-0027 to 2.02 µg/m^3 at Atlanta-0056, shown in Table 5. Providence-0030 had a high average BC concentration of 1.59 µg/m^3 and also had the highest UFP concentration out of the six sites that measured UFP. Of all sites used in this study (shown in Table 1), Providence-0030 was the site closest to the target roadway (5 meters away), likely leading to the higher particulate concentrations there compared to other sites.

BC concentrations followed a similar diurnal pattern across the sites. Average hourly BC concentrations peaked in the morning between 0600-0900 local time for all sites, a morning peak similar to the UFP diurnal pattern. Weekday concentrations were higher than weekend concentrations for all sites, with the weekday/weekend concentration ratio ranging from 1.13 at Columbus-0038 to 2.16 at Atlanta-0003. The sites with the highest weekday/weekend ratios typically had higher average BC concentrations—six of the seven sites with average BC concentrations above 1.5 µg/m^3 had weekday/weekend ratios above 1.6 (see the Appendix for the full relationship). The average BC values by hour of day and by weekday versus weekend are provided in the Appendix.

The distributions of BC while the near-road monitor was downwind of, parallel to, and upwind of the target roadway are shown in Figure 9. The median BC concentration was higher during downwind conditions than during parallel or upwind conditions for all sites except three: Berkeley-0013, Oakland-0012, and Fort Lee-0010. Berkeley and Oakland are impacted by the sea breeze effect; average wind speeds are ~2.5 times as high during downwind conditions as during upwind conditions, leading to greater dispersion and lower BC concentrations. BC concentrations do not have any noticeable variability during different wind directions at Fort Lee-0010. For the other 26 sites, we see a relationship similar to that shown in Figure 9, with downwind and parallel conditions leading to higher BC concentrations than upwind conditions. Median BC concentrations were 1.1 to 4.5 times higher under downwind conditions, compared to upwind conditions, for these 26 sites.

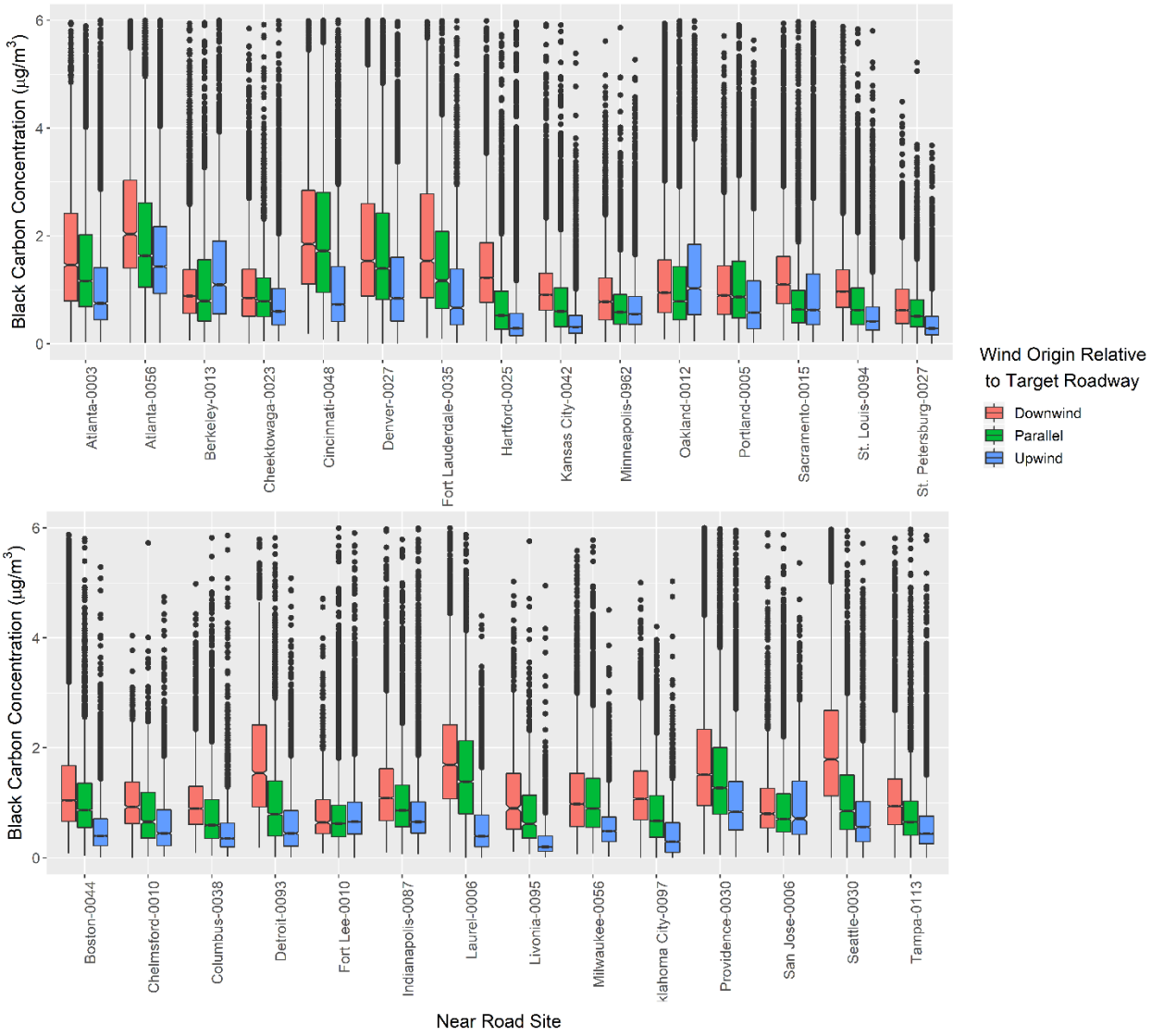

Figure 9. BC concentrations from 29 near-road sites under downwind, parallel, and upwind wind conditions during 2016-2018.

Table 5. Average BC concentrations and increments for the three-year period (2016-2018). Increments are calculated using the time series method by Wang et al. (2018) for all 29 sites and the nearby monitor (NM) method for 16 sites. The three-year average BC concentrations, increments, and roadway contributions are given for both time series and NM methods. Roadway contribution is calculated as the BC increment percentage of total average BC for sites with a positive increment.

Site Name	AQS ID	N hours Full Record	Time Series Three-Year Average (μg/m^3)	Time Series Increment (μg/m^3)	Time Series Roadway Contribution (%)	Nearby Monitor AQS ID	Distance to NM (km)	NM Three-Year Average (μg/m^3)	NM Increment (μg/m^3)	NM Roadway Contribution (%)
Denver-0027	08-031-0027	23204	1.75	1.04	59	NA	NA	NA	NA	NA
Atlanta-0003	13-089-0003	17482	1.91	0.96	50	NA	NA	NA	NA	NA
Atlanta-0056	13-121-0056	17481	2.02	0.92	46	NA	NA	NA	NA	NA
Fort Lauderdale-0035	12-011-0035	9784	1.71	0.91	53	NA	NA	NA	NA	NA
Cincinnati-0048	39-061-0048	26025	1.82	0.9	50	NA	NA	NA	NA	NA
Seattle-0030	53-033-0030	10367	1.5	0.82	55	53-033-0034	0.6	1.48	0.76	51
Providence-0030	44-007-0030	24305	1.59	0.75	47	44-007-0022	2.4	1.53	1.2	78
Oakland-0012	06-001-0012	24018	1.24	0.64	52	06-001-0011	2.9	1.18	0.52	44
Laurel-0006	24-027-0006	15871	1.31	0.61	46	24-033-0030	10.1	1.28	0.88	69
Berkeley-0013	06-001-0013	17159	1.16	0.57	49	06-001-0011	5.8	1.11	0.42	38
Detroit-0093	26-163-0093	8306	1.16	0.56	48	26-163-0033	13.1	1.22	0.48	39
Portland-0005	41-067-0005	16548	1.04	0.54	52	41-051-2010	19.3	1.01	0.39	39
Boston-0044	25-025-0044	25195	1.09	0.53	49	25-025-0042	2.2	1.06	0.43	41
Milwaukee-0056	55-079-0056	16298	1.03	0.51	49	55-079-0026	14.4	0.94	0.47	50
Sacramento-0015	06-067-0015	21827	1.03	0.49	47	06-067-0006	12	1.05	0.44	42
Indianapolis-0087	18-097-0087	19919	1.07	0.48	45	18-097-0078	2.9	1.04	0.45	43
Tampa-0113	12-057-0113	17790	0.89	0.47	53	12-103-0026	26.8	0.81	0.42	52
Hartford-0025	09-003-0025	52124	0.91	0.46	51	09-003-1003	4.3	0.87	0.4	46
San Jose-0006	06-085-0006	8025	0.99	0.46	46	06-001-0007	39.2	0.94	0.32	34

Site Name	AQS ID	N hours Full Record	Time Series Three-Year Average (µg/m^3)	Time Series Increment (µg/m^3)	Time Series Roadway Contribution (%)	Nearby Monitor AQS ID	Distance to NM (km)	NM Three-Year Average (µg/m^3)	NM Increment (µg/m^3)	NM Roadway Contribution (%)
Oklahoma City-0097	40-109-0097	14546	0.86	0.45	53	NA	NA	NA	NA	NA
Cheektowaga-0023	36-029-0023	16144	0.96	0.43	45	NA	NA	NA	NA	NA
St. Louis-0094	29-510-0094	25362	0.87	0.4	46	NA	NA	NA	NA	NA
Minneapolis-0962	27-053-0962	14367	0.79	0.4	50	NA	NA	NA	NA	NA
Chelmsford-0010	25-017-0010	4971	0.83	0.4	48	NA	NA	NA	NA	NA
Kansas City-0042	29-095-0042	24794	0.8	0.37	47	NA	NA	NA	NA	NA
Columbus-0038	39-049-0038	12124	0.8	0.36	45	NA	NA	NA	NA	NA
St. Petersburg-0027	12-103-0027	21994	0.62	0.34	54	12-103-0026	5.2	0.59	0.22	37
Fort Lee-0010	34-003-0010	24868	0.8	0.32	39	36-005-0110	6.8	0.78	-0.02	NA
Livonia-0095	26-163-0095	3580	0.62	0.28	46	NA	NA	NA	NA	NA

3.9.2 Black Carbon Increments

BC Increments are presented in Table 5 and **Figure 10** using two methods, the time series method developed by Wang et al. (2018) and the nearby monitor (NM) method. Time series increments are presented for all 29 sites. Of the 29 near-road sites with BC measurements, ambient measurements that were considered representative of background values were available for 16 sites; so NM increments were calculated for these 16 sites. Table 5 shows the average BC concentrations, increments, and ratios for the 29 sites. The time series increments ranged from 0.28 µg/m^3 at Livonia-0095 to 1.04 µg/m^3 at Denver-0027. The contribution of the roadway, calculated as the BC increment percentage of total average BC, had a range of 39% to 59% for time series increments as shown in Table 5. The NM BC increments were positive at all sites except Fort Lee-0010 (-0.02 µg/m^3). At the other 15 sites, BC increments ranged from 0.22 µg/m^3 at St. Petersburg-0027 to 1.2 µg/m^3 at Providence-0030. These positive NM increments corresponded to a roadway contribution range of 34% to 78%. A strong correlation was seen between the average BC concentration and the BC increment (R^2 = 0.72 for NM increments, R^2 = 0.95 for time series increments, see Appendix for additional figures). BC concentrations and increments were typically higher for sites closer to the roadway.

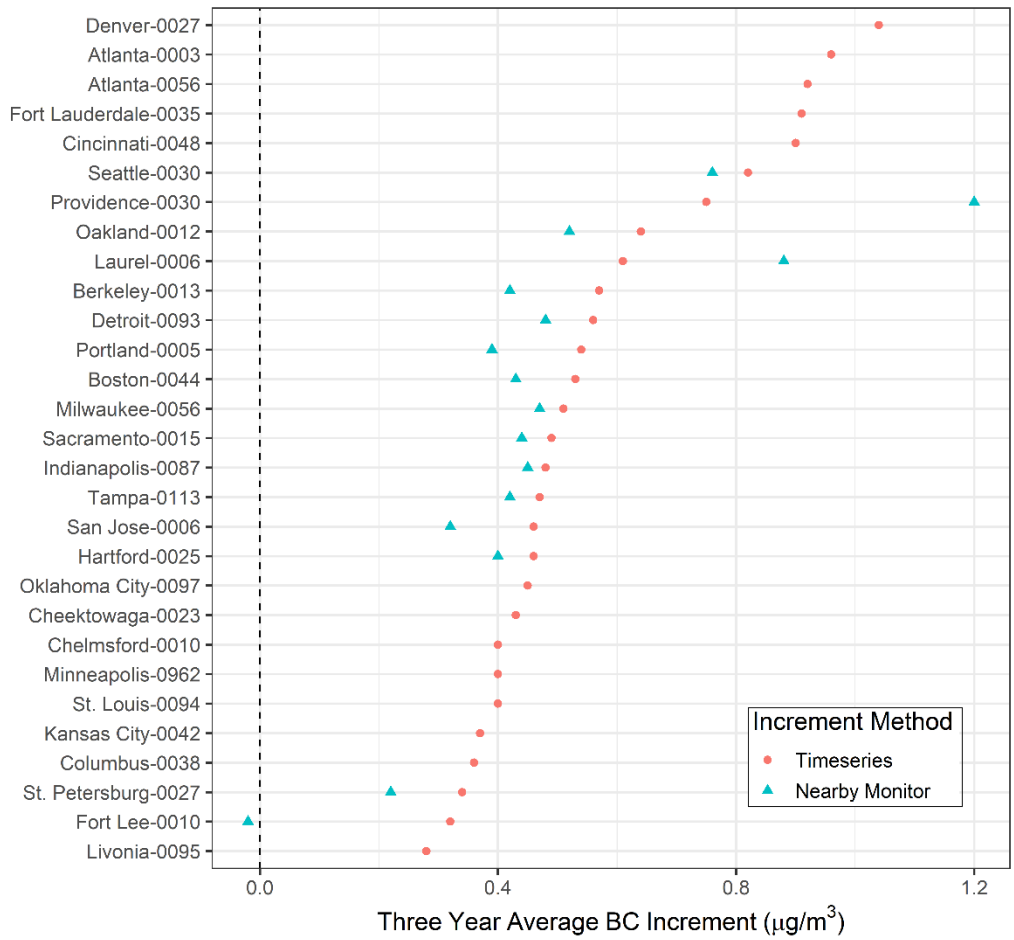

Figure 10. Three year average (2016-2018) BC increments calculated from the time series method developed by Wang et al. (2018) for all 29 sites and the nearby monitor method for 16 sites where nearby monitor data were available.

BC concentrations and increments were compared to the distance of the monitor to the roadway, traffic volume, and meteorology to see which variables had the strongest correlation. Pairwise R^2 values are shown in Table 6. The distance to road had the highest R^2 value for both BC concentrations and increments, showing a moderate correlation. AADT and FE-AADT show some correlation to BC concentration and increments. A weak correlation is seen for other variables. Table 6 can be compared with Table 3, which shows the analogous correlations with $PM_{2.5}$ increments. The monitor distance to road shows a greater R^2 correlation to both the BC concentration and the BC increment than the $PM_{2.5}$ increment. Some similarities are seen in the ranking of site variables when comparing Tables 3 and 6, with the monitor distance to road being the most correlated. FE-AADT, and AADT show some correlation to BC concentrations/increments and the $PM_{2.5}$ increment, whereas the percentage of time downwind has almost no correlation with either particulate increments. The relationships between the monitor distance to road and the BC concentration and increments are shown in Figure 11. Overall, there is modestly higher correlation of BC concentrations and

increments with distance to road than was seen for $PM_{2.5}$. As shown in Table 7, when using a linear regression to predict BC concentration or increment, there is a statistically significant relationship between distance to roadway and both BC concentration and BC increment (p-values less than 0.01). Weaker correlations are seen for other site variables.

Table 6. Coefficient of determination (R^2 value) of near-road site characteristics with BC concentrations and increments for 2016-2018. Only positive increments were used for pairwise R^2 values. Variables are rank-ordered by BC concentration R^2 values. All 29 sites were used for BC concentration and time series increments, and 16 sites were used for BC nearby monitor (NM) increments.

Variable	BC Concentration	BC NM Increment	BC Time Series Increment
Distance to Road	0.29	0.25	0.27
AADT	0.14	0.03	0.12
FE-AADT	0.12	0.10	0.07
Percent Parallel	0.11	0.02	0.09
Percent Upwind	0.08	0.02	0.10
Average Wind Speed	0.06	0.06	0.03
Percent Downwind	0.01	0.01	0.00

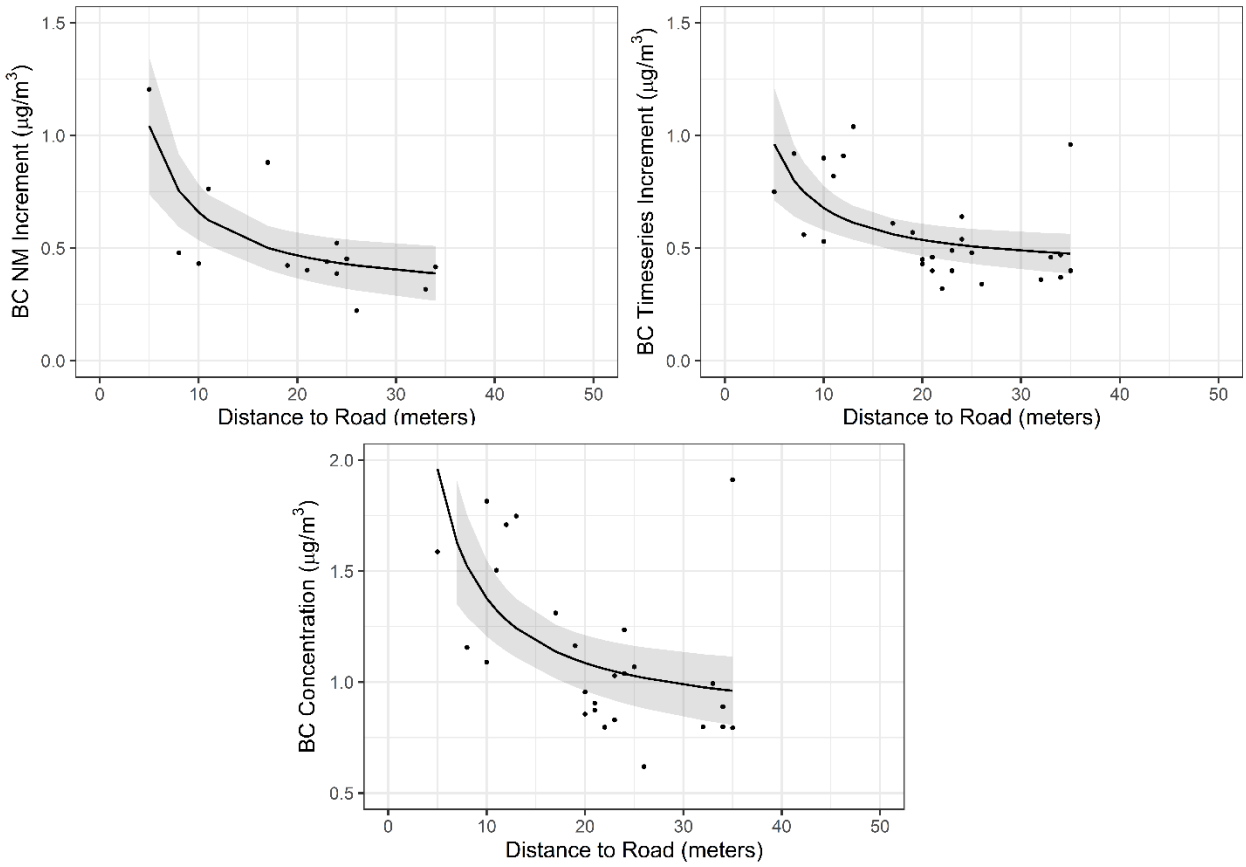

Figure 11. The relationship between the three year (2016-2018) average BC increment (top) and concentration (bottom) in comparison to distance to road. Regressions are shown in black, with the range of the standard error of the regression line shown in dark gray. All 29 sites were used for BC concentration and time series increments, and 16 sites were used for BC nearby monitor (NM) increments.

Table 7. The intercepts, slopes, p values, and R^2 values for linear regressions predicting BC concentration and increment with distance to road. For distance to road, an inverse relationship is used, of the form $y = a/x + b$.

Regression Model	Distance to Road vs. BC Concentration	Distance to Road vs. BC NM Increment	Distance to Road vs. BC Time Series Increment
N sites	29	16	29
a	5.82	3.84	2.83
b	0.80	0.28	0.39
p value	0.00046*	0.0018*	0.0022*
R^2	0.29	0.25	0.27

*Showing a greater than 99% statistical significance

3.9.3 Black Carbon Fraction of $PM_{2.5}$

Of the 29 near-road sites with BC measurements, $PM_{2.5}$ measurements from 20 of the sites had annual average $PM_{2.5}$ previously assessed. Table 8 presents 2018 annual average BC values, annual average $PM_{2.5}$ values, and the BC fraction of $PM_{2.5}$. The BC and $PM_{2.5}$ averages include contributions from both traffic-related emissions and ambient background concentrations. The BC fraction ranges from 6.1% at Fort Lee-0010 to 17.9% at Denver-0027. The BC fraction showed a strong relationship with distance to road (R^2 = 0.36), which is shown in Figure 12. Figure 12 shows a relationship that is consistent with the gradients of $PM_{2.5}$ and BC examined in the previous literature, such as (Karner et al., 2010). The BC fraction decreases with greater distance from the road because the BC increment is a substantial fraction of the total BC concentration (34% to 78% as shown in Table 5); in contrast, the $PM_{2.5}$ increment is a smaller fraction of the total $PM_{2.5}$ concentrations (1% to 27% as shown in Table 2). No statistically significant relationship was seen between BC fraction and FE-AADT (R^2 = 0.0008, p-value = 0.9).

Table 8. Annual average $PM_{2.5}$ and BC concentrations for 2018 for 20 near-road sites. Table is rank-ordered by BC fraction of $PM_{2.5}$.

Near-Road Site	BC Annual Average (μg/m^3)	$PM_{2.5}$ Annual Average (μg/m^3)	BC Fraction of $PM_{2.5}$ (%)	Distance to Road (m)	AADT	FE-AADT
Denver-0027	1.6	8.9	17.9	13	254,000	268,401
Fort Lauderdale-0035	1.7	9.3	17.8	12	300,000	609,962
Providence-0030	1.5	9	16.4	5	159,500	356,833
Portland-0005	1.2	7.7	16.1	24	162,700	301,466
Seattle-0030	1.4	9.4	15.1	11	167,093	332,515
Laurel-0006	1.2	9.2	12.6	17	199,131	482,296
Hartford-0025	0.8	7.2	11.6	21	164,300	238,235
Cincinnati-0048	1.4	12.2	11.3	10	152,115	360,578
Oklahoma City-0097	0.9	9.2	10	20	165,000	207,768
Minneapolis-0962	0.7	6.8	9.7	35	250,000	349,504
St. Louis-0094	0.8	8.6	9.4	21	147,943	334,351
Berkeley-0013	1.1	11.8	9.3	19	267,000	382,108
Indianapolis-0087	1	10.7	9	25	165,672	316,144
Boston-0044	0.9	10.3	8.8	10	205,861	261,441
Kansas City-0042	0.7	8.3	8.7	34	119,477	362,706
Oakland-0012	1.2	14.4	8.3	24	225,000	441,675
Columbus-0038	0.7	9.1	8	32	135,746	272,758
Sacramento-0015	0.9	12	7.7	23	190,800	487,258
San Jose-0006	0.9	12.1	7.5	33	251,000	386,540
Fort Lee-0010	0.7	11.3	6.1	22	282,912	556,501

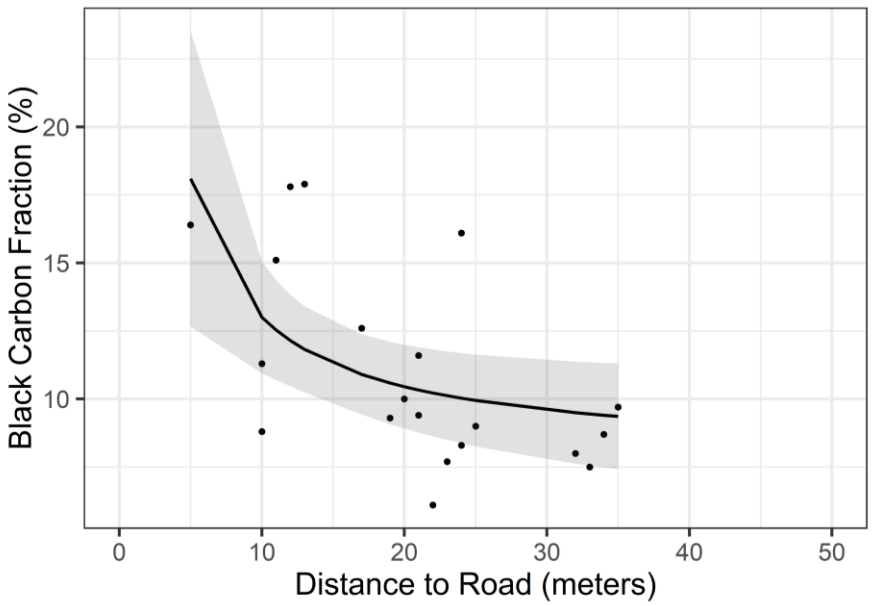

Figure 12. The relationship between the monitor distance to road and the BC fraction of $PM_{2.5}$, based on 2018 annual average values.

4. Conclusions

Near-road monitors stationed within 50 m of major roadways provide a novel resource to examine $PM_{2.5}$, BC, and UFP levels in the near-road environment. The near-road sites used in this study represent a diverse range of traffic and meteorology conditions. From an analysis of 32 near-road sites using 2018 measurements, after removing confounding site factors, the $PM_{2.5}$ increment values were below 2.0 μg/m^3, with the exception of one site (Laurel), which had an increment of 2.49 μg/m^3, based on FEM data. These increments corresponded to a roadway contribution between 1.3% and 27.1% of annual average $PM_{2.5}$. $PM_{2.5}$ increments derived from FRM data ranged from -0.14 ± 1.11 μg/m^3 to 1.68 ± 0.91 μg/m^3; uncertainty on the annual average increment was smaller for those derived from FRM data than for those derived from FEM data. $PM_{2.5}$ increments and BC increments were statistically related to some near-road site variables, and had the highest R^2 correlation with the monitor distance to road. Three other site variables showed statistical significance with $PM_{2.5}$ and BC increments in some cases: FE-AADT, percentage of time the monitor was upwind, and average wind speed. A clear relationship of higher median UFP and BC levels was seen during times when the monitor was downwind of the target roadway compared to upwind conditions. Diurnal patterns from 6 UFP stations and 29 BC stations showed a similar pattern, peaking during local morning hours for all sites. BC increments ranged from -0.02 to 1.2 μg/m^3. BC increments indicate a roadway contribution between 37% and 78% of total BC. Total BC ranged from 6.1% to 17.9% of total $PM_{2.5}$. This analysis provides evidence that particulate pollution decreases substantially within the first 50 meters of the roadway across a diverse range of major traffic roadways with high FE-AADT values (126,000 to 631,000).

5. References

Abu-Allaban M., Gillies J.A., Gertler A.W., Clayton R., and Proffitt D. (2007) Motor vehicle contributions to ambient PM_{10} and $PM_{2.5}$ at selected urban areas in the USA. *Environmental Monitoring and Assessment*, 132(1), 155-163, doi: 10.1007/s10661-006-9511-3. Available at https://doi.org/10.1007/s10661-006-9511-3.

Askariyeh M.H., Zietsman J., and Autenrieth R. (2019) Traffic contribution to $PM_{2.5}$ increment in the near-road environment. *Atmos. Environ.*, 117113, doi: 10.1016/j.atmosenv.2019.117113, 2019/11/07/. Available at http://www.sciencedirect.com/science/article/pii/S1352231019307526.

Baldwin N., Gilani O., Raja S., Batterman S., Ganguly R., Hopke P., Berrocal V., Robins T., and Hoogterp S. (2015) Factors affecting pollutant concentrations in the near-road environment. *Atmos. Environ.*, 115, 223-235, doi: http://doi.org/10.1016/j.atmosenv.2015.05.024. Available at http://www.sciencedirect.com/science/article/pii/S1352231015300972.

Brines M., Dall'Osto M., Beddows D.C.S., Harrison R.M., Gómez-Moreno F., Núñez L., Artíñano B., and others (2015) Traffic and nucleation events as main sources of ultrafine particles in high-insolation developed world cities. *Atmospheric Chemistry & Physics*, 15, 5929-5945, doi: 10.5194/acp-15-5929-2015, May 28. Available at http://www.atmos-chem-phys.net/15/5929/2015/acp-15-5929-2015.pdf.

Brown S.G., Penfold B.M., Mukherjee A., Landsberg K., and Eisinger D. (2019) Conditions leading to elevated $PM_{2.5}$ at near-road monitoring sites: case studies in Denver and Indianapolis. *International Journal of Environmental Research and Public Health*, 16(9), 1634, doi: 10.3390/ijerph16091634 (STI-7047), May 10. Available at https://www.mdpi.com/1660-4601/16/9/1634.

Canagaratna M.R., Onasch T.B., Wood E.C., Herndon S.C., Jayne J.T., Cross E.S., Miake-Lye R.C., Kolb C.E., and Worsnop D.R. (2010) Evolution of vehicle exhaust particles in the atmosphere. *J. Air Waste Manage.*, 60(10), doi: 10.3155/1047-3289.60.10.1192.

Clayton R., Gertler A.W., Proffitt D., Gillies J.A., and Abu-Allaban M. (2003) Particulate matter ($PM_{2.5}$ and PM_{10}) apportionment for on-road mobile sources. Final report prepared for the National Cooperative Research Program, Transportation Research Board, National Research Council, Washington, DC, Project HR-25-18, January.

Dabek-Zlotorzynska E., Celo V., Ding L., Herod D., Jeong C.-H., Evans G., and Hilker N. (2019) Characteristics and sources of $PM_{2.5}$ and reactive gases near roadways in two metropolitan areas in Canada. *Atmos. Environ.*, 218, December 1. Available at https://doi.org/10.1016/j.atmosenv.2019.116980.

de Jesus A.L., Rahman M.M., Mazaheri M., Thompson H., Knibbs L.D., Jeong C., Evans G., and others (2019) Ultrafine particles and $PM_{2.5}$ in the air of cities around the world: are they representative of each other? *Environment International*, 129, 118-135, doi: 10.1016/j.envint.2019.05.021. Available at http://www.sciencedirect.com/science/article/pii/S0160412019311110.

DeWinter J.L., Brown S.G., Seagram A.F., Landsberg K., and Eisinger D.S. (2018) A national-scale review of air pollutant concentrations measured in the U.S. near-road monitoring network during 2014 and 2015. *Atmos. Environ.*, 183, 94-105, doi: 10.1016/j.atmosenv.2018.04.003 (STI-6777), June.

Gertler A.W. (2005) Diesel vs. gasoline emissions: does PM from diesel or gasoline vehicles dominate in the US? *Atmos. Environ.*, 39(13), 2349-2355, doi: 10.1016/j.atmosenv.2004.05.065.

Harrison R.M., Beddows D.C., and Dall'Osto M. (2011) Source apportionment by PMF of wide range particle size spectra. *Geophysical Research Abstracts*, 13(EGU2011-7031).

Health Effects Institute (2013) Understanding the health effects of ambient ultrafine particles. Report prepared by the HEI Review Panel on Ultrafine Particles, Health Effects Institute, Boston, MA, January. Available at http://pubs.healtheffects.org/getfile.php?u=893.

Hilker N., Wang J.M., Jeong C.H., Healy R.M., Sofowote U., Debosz J., Su Y., Noble M., Munoz A., Doerksen G., White L., Audette C., Herod D., Brook J.R., and Evans G.J. (2019) Traffic-related air pollution near roadways: discerning local impacts from background. *Atmos. Meas. Tech.*, 12(10), 5247-5261, doi: 10.5194/amt-12-5247-2019. Available at https://www.atmos-meas-tech.net/12/5247/2019/.

Holmes N.S. (2007) A review of particle formation events and growth in the atmosphere in the various environments and discussion of mechanistic implications. *Atmos. Environ.*, 41(10), 2183-2201, doi: 10.1016/j.atmosenv.2006.10.058. Available at http://www.sciencedirect.com/science/article/pii/S1352231006010934.

Janssen N.A.H., Gerlofs-Nijland M.E., Lanki T., Salonen R.O., Cassee F., Hoek G., Fischer P., Brunekreef B., and Krzyzanowski M. (2012) Health effects of black carbon. Report by World Health Organization Regional Office for Europe, ISBN: 978 92 890 0265 3. Available at http://www.euro.who.int/en/health-topics/environment-and-health/air-quality/publications/2012/health-effects-of-black-carbon-2012.

Jeong C.-H., Wang J.M., Hilker N., Debosz J., Sofowote U., Su Y., Noble M., Healy R.M., Munoz T., Dabek-Zlotorzynska E., Celo V., White L., Audette C., Herod D., and Evans G.J. (2019) Temporal and spatial variability of traffic-related $PM_{2.5}$ sources: comparison of exhaust and non-exhaust emissions. *Atmos. Environ.*, 198, 55-69, doi: 10.1016/j.atmosenv.2018.10.038, 2019/02/01/. Available at http://www.sciencedirect.com/science/article/pii/S1352231018307283.

Karner A., Eisinger D.S., and Niemeier D. (2010) Near-roadway air quality: synthesizing the findings from real-world data. *Environ. Sci. Technol.*, 44, 5334-5344, doi: 10.1021/es100008x (STI-3923). Available at http://pubs.acs.org/doi/abs/10.1021/es100008x.

Kleeman M.J., Riddle S.G., Robert M.A., Jakober C.A., Fine P.M., Hays M.D., Schauer J.J., and Hannigan M.P. (2009) Source apportionment of fine ($PM_{1.8}$) and ultrafine ($PM_{0.1}$) airborne particulate matter during a severe winter pollution episode. *Environ. Sci. Technol.*, 43(2), 272-279, doi: 10.1021/es800400m, January. Available at http://dx.doi.org/10.1021/es800400m.

Kulmala M., Vehkamaki H., Petäjä T., Dal Maso M., Lauri A., Kerminen V.M., Birmili W., and McMurry P.H. (2004) Formation and growth rates of ultrafine atmospheric particles: a review of observations. *Journal of Aerosol Science*, 35(2), 143-176, doi: 10.1016/j.jaerosci.2003.10.003, Feb. Available at http://www.sciencedirect.com/science/article/pii/S0021850203004373.

Kumar P., Morawska L., Birmili W., Paasonen P., Hu M., Kulmala M., Harrison R.M., Norford L., and Britter R. (2014) Ultrafine particles in cities. *Environment International*, 66, 1-10, doi: 10.1016/j.envint.2014.01.013, May. Available at http://www.sciencedirect.com/science/article/pii/S016041201400018X?np=y.

Long C.M., Nascarella M.A., and Valberg P.A. (2013) Carbon black vs. black carbon and other airborne materials containing elemental carbon: Physical and chemical distinctions. *Environmental Pollution*, 181, 271-286, October 2013. Available at https://doi.org/10.1016/j.envpol.2013.06.009.

Marmur A., Park S.K., Mulholland J.A., Tolbert P.E., and Russell A.G. (2006) Source apportionment of $PM_{2.5}$ in the southeastern United States using receptor and emissions-based models: conceptual differences and implications for time-series health studies. *Atmos. Environ.*, 40(14), 2533-2551, May.

Morawska L., Ristovski Z., Jayaratne E.R., Keogh D.U., and Ling X. (2008) Ambient nano and ultrafine particles from motor vehicle emissions: characteristics, ambient processing and implications on human exposure. *Atmos. Environ.*, 42, 8113-8138, November. Available at http://www.sciencedirect.com/science/article/pii/S1352231008006961.

Mukherjee A., McCarthy M.C., Brown S.G., Huang S., Landsberg K., and Eisinger D.S. (2019) Influence of roadway emissions on near-road $PM_{2.5}$: monitoring data analysis and implications for determining transportation projects of local air quality concern (POAQC). Final report prepared for the Washington State Department of Transportation, lead agency for the Near-Road Air Quality Research Transportation Pooled Fund, by Sonoma Technology, Inc., Petaluma, CA, STI-914203-7088, July.

Németh Z., Rosati B., Zíková N., Salma I., Bozó L., Dameto de España C., Schwarz J., Ždímal V., and Wonaschütz A. (2018) Comparison of atmospheric new particle formation events in three Central European cities. *Atmos. Environ.*, 178, 191-197, doi: 10.1016/j.atmosenv.2018.01.035.

Riddle S.G., Robert M.A., Jakober C.A., Hannigan M.P., and Kleeman M.J. (2008) Size-resolved source apportionment of airborne particle mass in a roadside environment. *Environ. Sci. Technol.*, 42(17), 6580-6586, doi: 10.1021/es702827h.

Robinson A.L., Donahue N.M., Shrivastava M.K., Weitkamp E.A., Sage A.M., Grieshop A.P., Lane T.E., Pierce J.R., and Pandis S.N. (2007) Rethinking organic aerosols: semivolatile emissions and photochemical aging. *Science*, 315, 1259.

Rowangould G.M. (2013) A census of the US near-roadway population: public health and environmental justice considerations. *Transportation Research Part D: Transport and Environment*, 25, 59-67.

Salma I., Borsós T., Németh Z., Weidinger T., Aalto P., and Kulmala M. (2014) Comparative study of ultrafine atmospheric aerosol within a city. *Atmos. Environ.*, 92, 154-161, doi: 10.1016/j.atmosenv.2014.04.020, August. Available at http://www.sciencedirect.com/science/article/pii/S1352231014002921.

Seagram A., Huang S., Brown S., Landsberg K., DeWinter J., and Eisinger D. (2019a) National assessment of near-road air quality: trends and estimation of near-road $PM_{2.5}$ increment. Presented at the Transportation Research Board 2019 Annual Meeting, Analysis Subcommittee, Transportation and

Air Quality Committee, Washington, DC, January 14, by Sonoma Technology, Inc., Petaluma, CA. STI-7034.

Seagram A.F., Brown S.G., Huang S., Landsberg K., and Eisinger D.S. (2019b) National assessment of near-road air quality in 2016: multi-year pollutant trends and estimation of near-road $PM_{2.5}$ increment. *Transportation Research Record*, doi: 10.1177/0361198119825538 (STI-6963), January 30. Available at https://journals.sagepub.com/doi/10.1177/0361198119825538.

Sofowote U.M., Healy R.M., Su Y., Debosz J., Noble M., Munoz A., Jeong C.-H., Wang J.M., Hilker N., Evans G.J., and Hopke P.K. (2018) Understanding the $PM_{2.5}$ imbalance between a far and near-road location: Results of high temporal frequency source apportionment and parameterization of black carbon. *Atmos. Environ.*, 173, 277-288. Available at https://www.sciencedirect.com/science/article/pii/S1352231017307367.

U.S. Environmental Protection Agency (2010) Final revisions to the primary national ambient air quality standard for nitrogen dioxide. January, presented by the Office of Air and Radiation and the Office of Air Quality Planning and Standards. Available at http://www.epa.gov/apti/video/pdfs/NO2%20overview%20presentation%20012410.pdf.

U.S. Environmental Protection Agency (2012) Near-road NO_2 monitoring: technical assistance document. EPA-454/B-12-002, June. Available at http://www.epa.gov/ttn/amtic/nearroad.html.

U.S. Environmental Protection Agency (2015a) Transportation conformity guidance for quantitative hot-spot analyses in $PM_{2.5}$ and PM_{10} nonattainment and maintenance areas. Prepared by the EPA Office of Transportation and Air Quality, Transportation and Climate Division, Washington, DC, EPA-420-B-15-084, November. Available at https://nepis.epa.gov/Exe/ZyPDF.cgi?Dockey=P100NMXM.pdf, appendix available at https://nepis.epa.gov/Exe/ZyPdf.cgi?Dockey=P100NN22.pdf.

U.S. Environmental Protection Agency (2015b) 3-year quality assurance report for calendar years 2011, 2012, and 2013: $PM_{2.5}$ ambient air monitoring program. EPA-454/R-15-002, March. Available at https://www3.epa.gov/ttnamti1/files/ambient/pm25/qa/20112013pm25qareport.pdf.

Venecek M.A., Yu X., and Kleeman M.J. (2019) Predicted ultrafine particulate matter source contribution across the continental United States during summertime air pollution events. *Atmos. Chem. Phys.*, 19(14), 9399-9412, doi: 10.5194/acp-19-9399-2019. Available at https://www.atmos-chem-phys.net/19/9399/2019/.

Wang Y., Hopke P.K., and Utell M.J. (2011) Urban-scale spatial-temporal variability of black carbon and winter residential wood combustion particles. *Aerosol and Air Quality Research*, 11, 473-481, doi: 10.4029/aaqr.2011.01.0005. Available at http://aaqr.org/VOL11_No5_October2011/1_AAQR-11-01-OA-0005_473-481.pdf.

Wang Z., Zhong S., He H.-d., Peng Z.-R., and Cai M. (2018) Fine-scale variations in $PM_{2.5}$ and black carbon concentrations and corresponding influential factors at an urban road intersection. *Building and Environment*, 141, 215-225, doi: 10.1016/j.buildenv.2018.04.042, August 15. Available at http://www.sciencedirect.com/science/article/pii/S0360132318302531.

Zhu Y.F., Hinds W.C., Kim S., and Sioutas C. (2002) Concentration and size distribution of ultrafine particles near a major highway. *J. Air Waste Manage.*, 52(9), 1032-1042, September.

Appendix: Supplementary Data

This appendix shows the diurnal pattern of UFP particles, the weekday versus weekend distributions of UFP particles, average BC concentrations by weekday, weekend, and three-hour periods, the relationship between average BC and the BC weekday/weekend ratio, the relationship between the BC increment and total BC, and the full range of $PM_{2.5}$ increment uncertainty for all 46 near road sites.

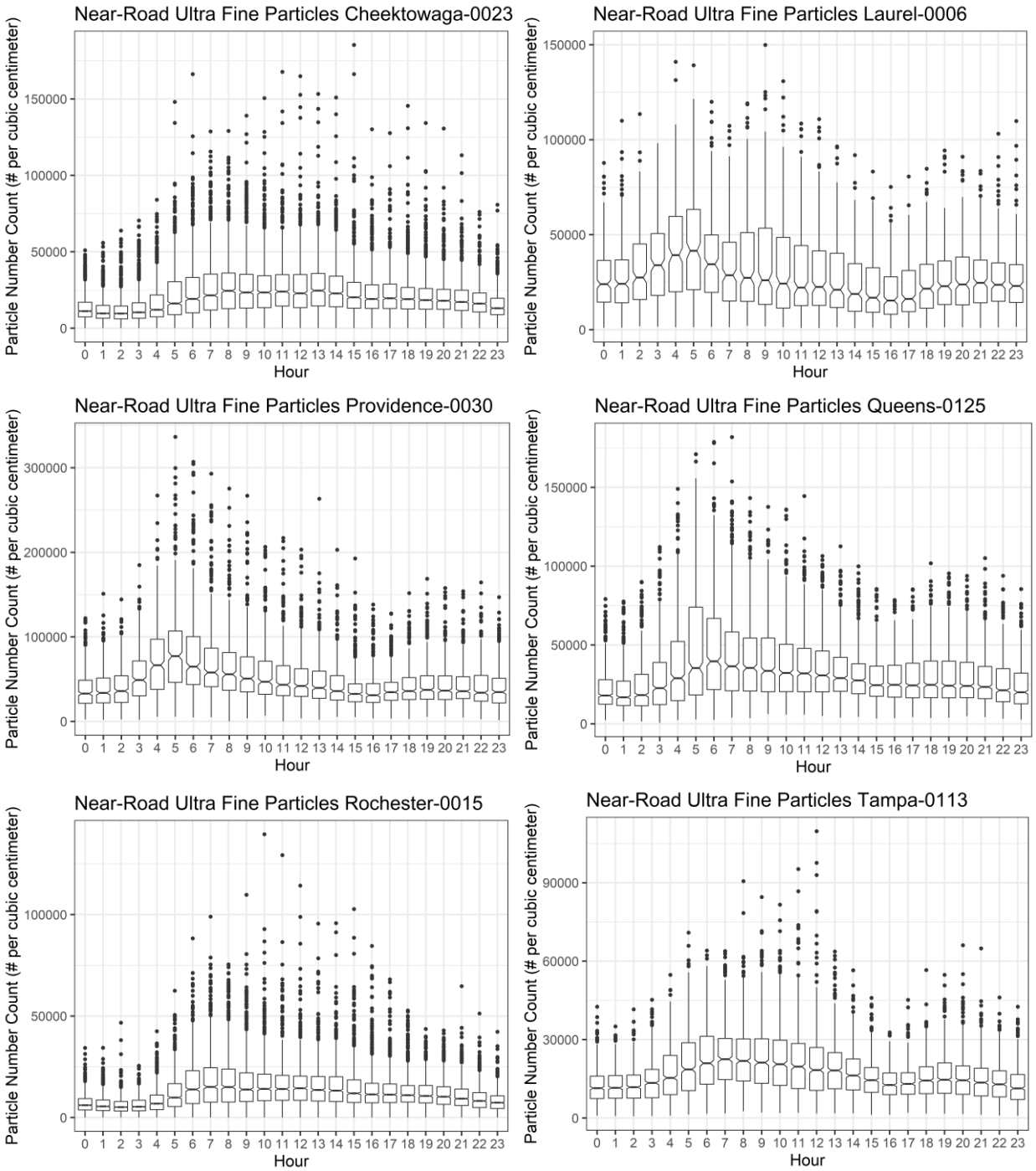

Figure A-1. UFP number count boxplot distributions by local hour of day for 2016-2018. The center of the box plot represents the median value. The box cutoffs are the inter-quartile ranges (IQRs), the line segments represent 1.5 x IQR, and the remaining points in the distribution are plotted individually.

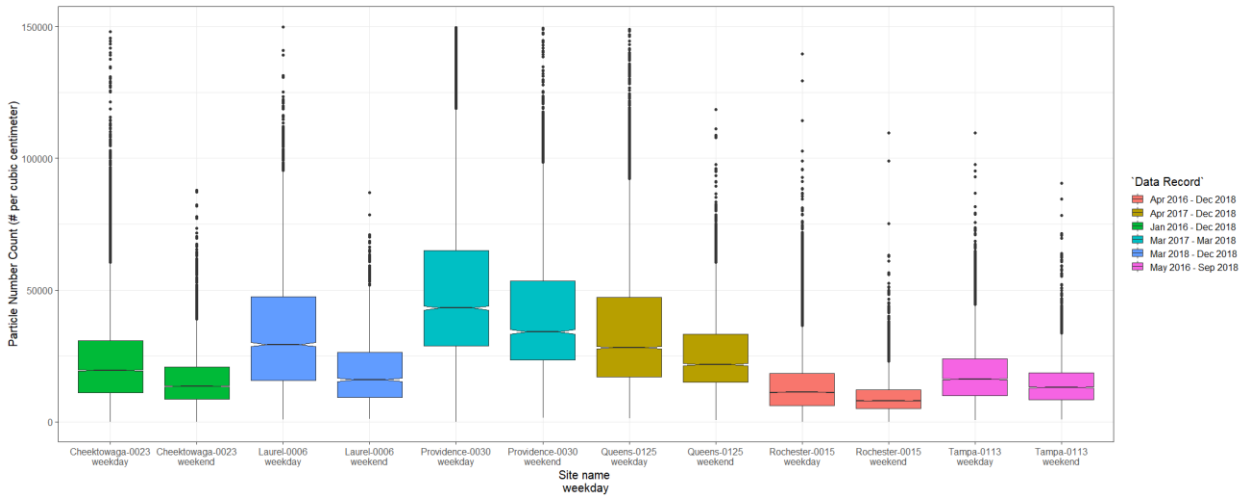

Figure A-2. UFP number count boxplot distributions for weekday and weekend periods for 2016-2018.

Table A-1. Average 2016-2018 BC concentrations by selected time interval. All values have the units µg/m^3.

Near-Road Site	Three year	Mon-Fri	Sat & Sun	Hour 0-2	Hour 3-5	Hour 6-8	Hour 9-11	Hour 12-14	Hour 15-17	Hour 18-20	Hour 21-23
Oakland-0012	1.24	1.36	0.94	0.80	0.95	1.70	1.88	1.45	1.13	1.00	0.98
Berkeley-0013	1.16	1.28	0.86	0.74	1.01	1.60	1.67	1.27	1.01	1.06	0.95
Sacramento-0015	1.03	1.10	0.85	0.90	0.97	1.25	1.10	1.00	0.95	1.00	1.05
San Jose-0006	0.99	1.07	0.79	NA	NA	1.34	1.03	0.87	0.84	0.89	0.98
Denver-0027	1.75	2.00	1.12	1.00	1.60	3.00	2.10	1.95	1.59	1.45	1.24
Hartford-0025	0.91	1.04	0.58	0.67	0.93	1.37	0.99	0.88	0.83	0.80	0.76
Fort Lauderdale-0035	1.71	2.00	0.98	0.89	1.39	2.53	2.38	2.33	1.78	1.38	1.01
Tampa-0113	0.89	0.97	0.68	0.79	1.09	1.54	0.78	0.64	0.70	0.80	0.78
St. Petersburg-0027	0.62	0.67	0.49	0.54	0.77	1.06	0.69	0.53	0.41	0.44	0.51
Atlanta-0003	1.91	2.26	1.05	2.10	2.51	2.59	1.70	1.35	1.32	1.76	1.96
Atlanta-0056	2.02	2.23	1.52	1.45	1.92	2.83	2.86	2.24	1.62	1.61	1.66
Indianapolis-0087	1.07	1.13	0.91	1.01	1.05	1.33	1.00	0.88	0.95	1.12	1.22

Near-Road Site	Three year	Mon-Fri	Sat & Sun	Hour 0-2	Hour 3-5	Hour 6-8	Hour 9-11	Hour 12-14	Hour 15-17	Hour 18-20	Hour 21-23
Laurel-0006	1.31	1.49	0.86	1.35	1.66	1.83	1.32	1.01	0.92	1.14	1.25
Chelmsford-0010	0.83	0.93	0.59	0.73	0.89	1.06	0.78	0.76	0.80	0.82	0.81
Boston-0044	1.09	1.24	0.71	0.78	1.28	1.76	1.42	1.01	0.81	0.84	0.84
Detroit-0093	1.16	1.30	0.79	0.80	1.00	1.67	1.47	1.32	1.20	0.91	0.87
Livonia-0095	0.62	0.68	0.49	0.50	0.50	0.78	0.69	0.57	0.62	0.72	0.62
Minneapolis-0962	0.79	0.85	0.65	0.61	0.75	1.12	0.93	0.80	0.68	0.71	0.75
Kansas City-0042	0.8	0.84	0.70	0.70	0.75	0.96	0.74	0.70	0.78	0.91	0.85
St. Louis-0094	0.87	0.94	0.71	0.80	0.88	1.29	0.95	0.82	0.63	0.76	0.87
Fort Lee-0010	0.8	0.90	0.54	0.67	0.90	1.12	0.92	0.74	0.64	0.69	0.69
Cheektowaga-0023	0.96	1.02	0.80	0.88	0.88	1.14	0.87	0.85	0.93	0.98	1.12
Columbus-0038	0.8	0.83	0.73	0.73	0.75	1.08	0.79	0.67	0.67	0.81	0.89
Cincinnati-0048	1.82	2.06	1.21	1.68	2.12	2.80	1.98	1.44	1.21	1.57	1.72
Oklahoma City-0097	0.86	0.93	0.68	0.54	0.63	1.09	0.98	0.98	1.00	0.90	0.73
Portland-0005	1.04	1.18	0.68	0.79	0.97	1.40	1.14	1.06	0.98	1.02	0.95
Providence-0030	1.59	1.80	1.07	1.20	1.93	2.48	1.79	1.55	1.26	1.23	1.26
Seattle-0030	1.5	1.72	0.97	0.85	1.17	1.99	2.24	1.86	1.52	1.31	1.10
Milwaukee-0056	1.03	1.15	0.73	0.79	1.17	1.59	1.07	0.92	0.92	0.88	0.89

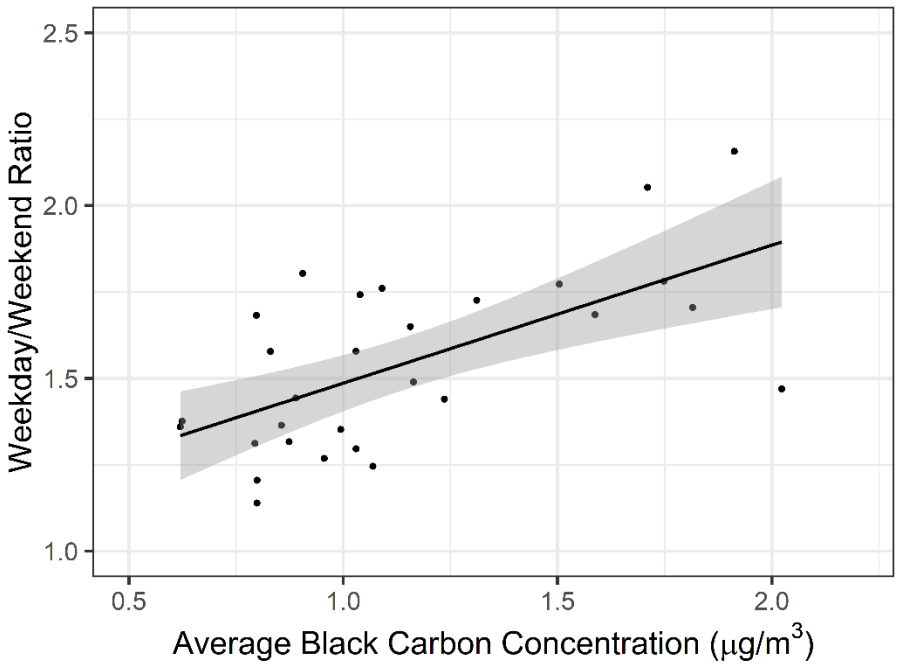

Figure A-3. The relationship between three-year (2016-2018) average BC concentrations with the ratio of average weekday to average weekend concentrations. Regressions are shown in black, with the range of the standard error of the regression line shown in dark gray.

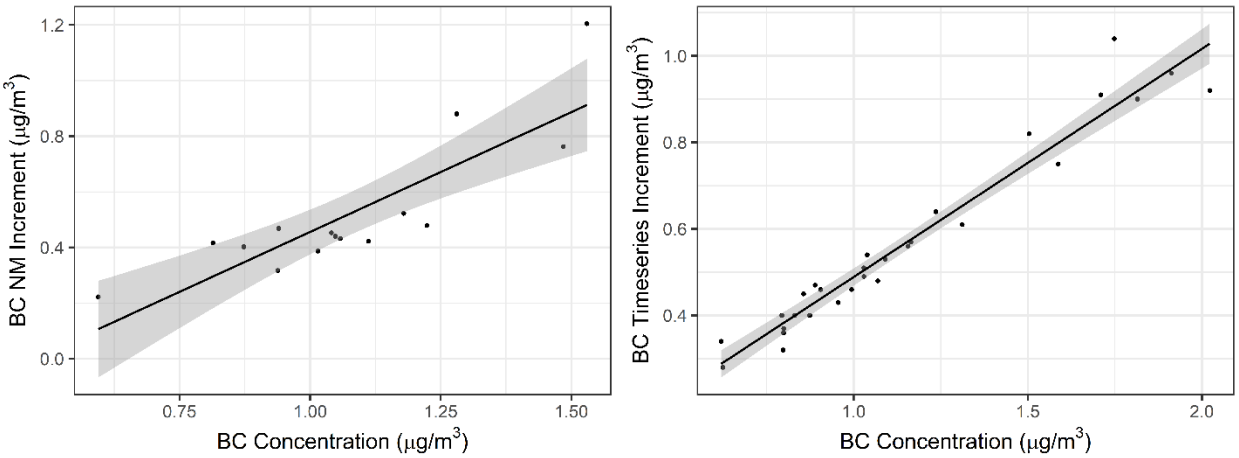

Figure A-4. The relationship between the three-year (2016-2018) average BC increment and the three-year (2016-2018) average BC concentration.

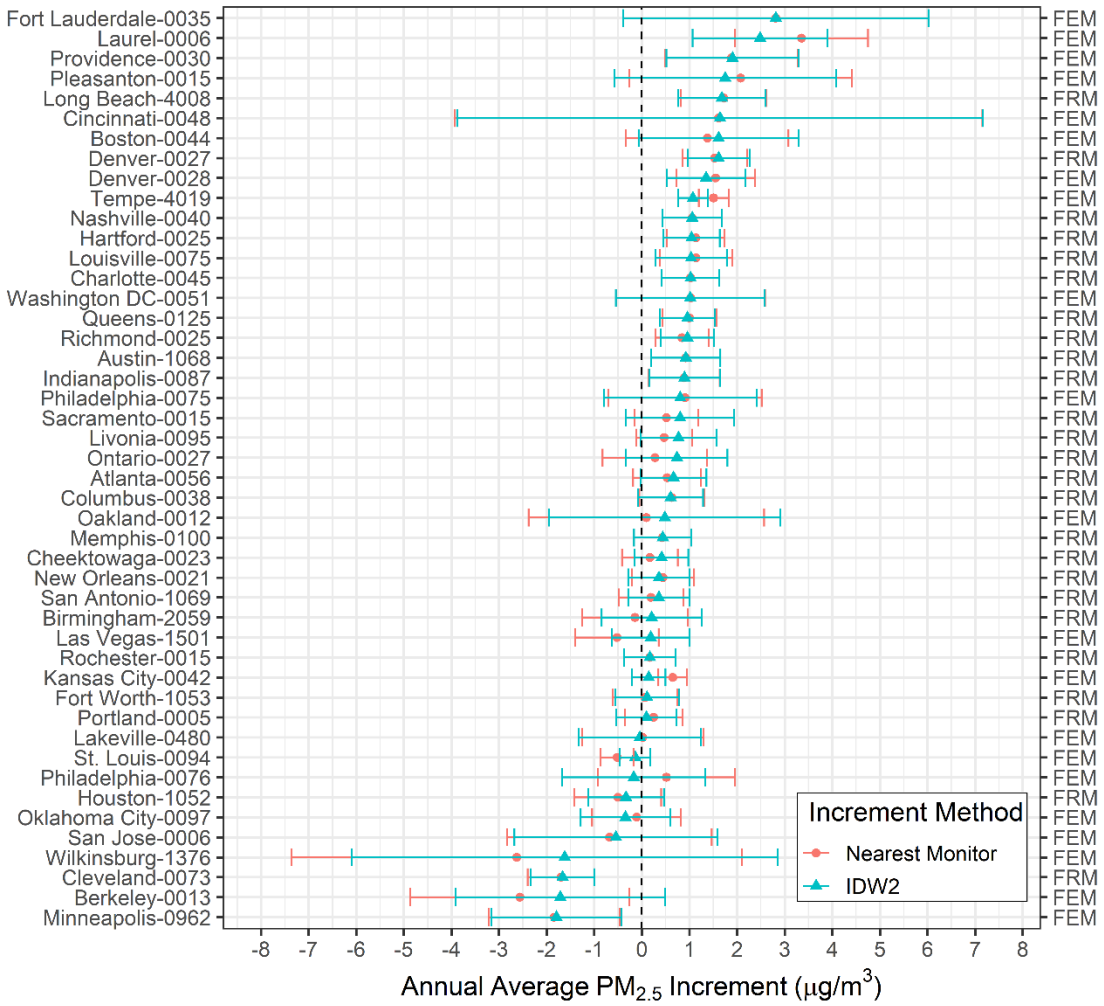

Figure A-5. Distributions of 2018 annual average $PM_{2.5}$ increments using identical instrument methods from 46 near-road sites, computed using IDW and the nearest-monitor method. The instrument measurement type (FRM vs FEM) is shown for each site. Uncertainty bars represent instrument bias and statistical uncertainty of the mean. The same data and visualization is shown in Figure 4, but the full range of uncertainty bars is included here.

Table A-2. Annual average $PM_{2.5}$ concentrations from 26 near-road sites based on data from the 2016 to 2018 period. All $PM_{2.5}$ concentration values have the units $\mu g/m^3$. Three-year trend is the slope of regression, with units of $\mu g/m^3$ per year. Sites are rank ordered by three-year (2016-2018) average $PM_{2.5}$.

Near-Road Site	State	2016 Mean $PM_{2.5}$	2017 Mean $PM_{2.5}$	2018 Mean $PM_{2.5}$	3-Year Mean $PM_{2.5}$	AADT	FE-AADT	Distance to Road	3-Year Trend
Ontario-0027	CA	14.9	14.6	14.5	14.6	217,000	631,557	18	-0.2
Long Beach-4008	CA	12.0	12.8	13.2	12.7	190,000	612,560	24	0.6
Oakland-0012	CA	8.8	11.7	14.4	11.6	225,000	441,675	24	2.8
San Jose-0006	CA	9.2	10.9	12.1	10.7	251,000	386,540	33	1.45
Wilkinsburg-1376	PA	10.7	10.7	10.3	10.6	74,421	126,040	23	-0.2
Birmingham-2059	AL	10.8	10.3	10.2	10.4	126,670	193,362	25	-0.3
Indianapolis-0087	IN	10.1	9.6	10.7	10.1	165,672	316,144	25	0.3
Louisville-0075	KY	9.2	8.9	10.2	9.4	188,697	286,634	33	0.5
Denver-0028	CO	9.6	8.9	9.2	9.2	230,000	252,563	16	-0.2
Laurel-0006	MD	9.8	8.4	9.2	9.1	199,131	482,296	17	-0.3
Philadelphia-0075	PA	9.4	8.1	9.7	9.1	118,498	244,832	14	0.15
Providence-0030	RI	9.3	8.3	9.0	8.9	159,500	356,833	5	-0.15
Livonia-0095	MI	8.5	8.4	9.1	8.7	193,400	313,407	56	0.3
St. Louis-0094	MO	8.8	8.4	8.6	8.6	147,943	334,351	21	0
Fort Worth-1053	TX	8.5	8.6	8.5	8.6	159,040	209,139	38	-0.1
Boston-0044	MA	6.9	7.8	10.3	8.3	205,861	261,441	10	1.7
Tempe-4019	AZ	8.0	8.1	8.7	8.2	267,488	521,640	13	0.35
Denver-0027	CO	7.8	7.9	8.3	8.0	254,000	268,401	13	0.25
New Orleans-0021	LA	7.5	8.1	8.4	8.0	98,800	187,721	32	0.45
Minneapolis-0962	MN	7.9	7.7	6.8	7.5	250,000	349,504	35	-0.55

Near-Road Site	State	2016 Mean $PM_{2.5}$	2017 Mean $PM_{2.5}$	2018 Mean $PM_{2.5}$	3-Year Mean $PM_{2.5}$	AADT	FE-AADT	Distance to Road	3-Year Trend
Kansas City-0042	MO	6.2	7.8	8.3	7.4	119,477	362,706	34	1.05
Portland-0005	OR	6.2	7.9	7.7	7.3	162,700	301,466	24	0.4
Hartford-0025	CT	7.6	7.1	7.2	7.3	164,300	238,235	21	-0.2
Cheektowaga-0023	NY	6.8	7.4	7.6	7.3	126,107	212,275	20	0.75
Rochester-0015	NY	6.3	6.7	7.4	6.8	98,306	128,179	11	0.55
Lakeville-0480	MN	5.7	6.1	7.4	6.4	83,000	184,317	34	0.85